Ulrich Wohlgenannt, BSc

High Parallel Optical Test

MASTER'S THESIS

to achieve the university degree of
Diplom-Ingenieur

Master's degree programme: Technical Physics

submitted to

Graz University of Technology

Supervisor

Ao.Univ.-Prof. Dipl.-Ing. Dr.techn. Gernot Pottlacher

Institute of Experimental Physics

in cooperation with ams AG

Graz, June 2017

AFFIDAVIT

I declare that I have authored this thesis independently, that I have not used other than the declared sources/resources, and that I have explicitly indicated all material which has been quoted either literally or by content from the sources used. The text document uploaded to TUGRAZonline is identical to the present master‘s thesis.

Date

Signature

Acknowledgements

I want to thank my supervisor from TU Graz Prof. Gernot Pottlacher, who accompanied me throughout my thesis. He and his team always supported me with curiosity and advice. My special appreciation goes to my supervisor at ams AG, Curd Trattler who did not get tired of talking shop with me. I learned a lot during our talks and my fascination for the topic grew every single time.

Furthermore I want to thank Steve Mitchell, Werner Rauch and Mario Manninger. Our meetings were a pleasure and I could always count on their positive and helpful contribution. Also I want to thank my other colleagues and fellow students. The mixture of expertise, joy and friendship is the key to a successful professional life and I am glad that I found many people who shared this path with me.

My studies wouldn't have been possible without my friends who kept my moral high and let me feel that they believe in what I'm doing. Especially Andrea didn't only share her experience with me, she was also a pillar I could always count on.

Above all I want to thank my family and especially my parents who supported me in any possible way. They always believed in me, in good and especially in bad times. I will always be grateful for that.

Abstract

Colour sensors are used in many applications nowadays. Since the production volume is very high and the sensors must be sufficiently exact, calibration is a challenge. This thesis discusses the attempt to calibrate numerous colour sensors using an integrating sphere with one meter diameter. With this method multiple sensors can be calibrated using the same calibration lamps and only one reference spectrometer. To provide a variety of light situations many different calibration lamps must be used. The lamp type and the colour temperature of the emitted light are the two significant factors regarding the lamp selection. 16 lamps are used in the described experimental setup. They are mounted on a lamp frame inside the integrating sphere and can be switched and dimmed individually. To generate equal light conditions for each sensor, the light homogeneity provided by the integrating sphere is of major effect. For the calibration of colour sensors particularly the chromaticity homogeneity is of interest. The two colour difference magnitudes CIEDE2000 and the distance in the CIE (u'v') chromaticity diagram are used to evaluate the integrating spheres performance. The data for the evaluation are collected by measuring a grid of coordinates in the integrating spheres 254 mm (10 inch) light exit port. A spectrometer probe is moved to every pair of grid coordinates in the port plain and the corresponding tristimulus values are measured. Since integrating spheres have excellent diffusive properties, the required colour homogeneity could be achieved easily. Chromaticity differences generally fell below the limits by a factor of 10. The second property to investigate was the performance of the experimental setup when a sensor is calibrated. For most lamps the measured chromaticity difference between the calibrated and the uncalibrated test sensor fell below the limits. Fluorescent lamps were a challenge for the calibration. A less general selection of lamps made a good calibration possible and led to results of satisfying accuracy.

Kurzfassung

Farbsensoren finden seit einigen Jahren ein zunehmend breites Spektrum an Anwendungen. Da die Stückzahlen in der Produktion sehr hoch sind, verursacht die Kalibrierung der Sensoren einen großen Aufwand. Diese Masterarbeit untersucht die Eignung einer Ulbrichtkugel mit einem Meter Durchmesser für die Kalibrierung. Dadurch wird es möglich, mit einem Referenzspektrometer viele Sensoren gleichzeitig zu kalibrieren. Um die Sensoren für eine Vielzahl von Lichtverhältnissen vorzubereiten, müssen mehrere Kalibrierlampen verwendet werden. Bei der Auswahl kommt es besonders auf den Typ der Lampen, sowie auf ihre Farbtemperatur an. Der in dieser Arbeit beschriebene experimentelle Aufbau ermöglicht die Verwendung von 16 Kalibrierlampen. Diese werden auf einem Lampenring im Inneren der Kugel befestigt und können individuell angesteuert und gedimmt werden. Um für alle Sensoren dieselben Lichtverhältnisse bereitzustellen, ist es wichtig eine homogene Ausleuchtung des Lichtaustrittsschachts zu erzeugen. Insbesondere die Homogenität der Farbart ist für die Kalibrierung von Farbsensoren maßgeblich. Für die Bewertung werden der CIEDE2000 Farbunterschied, sowie der Abstand im CIE (u'v') Farbdiagramm herangezogen. Die Messdaten werden von einer beweglichen Spektrometersonde gesammelt, die verschiedene Gitterpunkte in der Ebene des 254 mm (10 zoll) Lichtaustrittsschachts ansteuert. An jedem Koordinatenpunkt wird eine Tristimulus-Messung durchgeführt. Da Ulbrichtkugeln allgemein eine sehr gute Lichtstreuung erzeugen, konnte die gewünschte Lichthomogenität leicht erreicht werden. Die Grenze für den Farbunterschied wurde zirka um den Faktor 10 unterschritten. Neben der Farbhomogenität wird weiters untersucht, wie sich der experimentelle Aufbaus bei der Sensorkalibrierung verhält. Mit dem Testsensor konnten auch hier sehr gute Ergebnisse erzielt werden. Der gemessene Farbunterschied vom kalibrierten zum unkalibrierten Sensor lag für die meisten Lampen unter dem geforderten Grenzwert. Fluoreszenzlampen waren für die Kalibrierung eine Herausforderung. Durch eine weniger allgemeine Lampenselektion konnten sie jedoch in die Kalibrierung einbezogen und vom Sensor mit zufriedenstellender Genauigkeit gemessen werden.

Contents

List of Figures

List of Tables

Nomenclature

λ	Electromagnetic wavelength
$S_\lambda(\lambda)$	Spectral energy
$\overline{x}(\lambda)$, $\overline{y}(\lambda)$, $\overline{z}(\lambda)$	CIE standard observer color matching functions
(X, Y, Z)	Tristimulus values
(X_r, Y_r, Z_r)	Reference white for CIELAB transformation
L, a, b	CIELAB color coordinates
u', v'	CIE(u'v') chromaticity coordinates
ΔE_{00}	CIEDE2000 color difference
$\Delta_{u'v'}$	Distance in the CIE (u'v') chromaticity diagram
d_{ref}, d_{port}	Distance of a certain measurement from the reference measurement. The reference point is generally the probe port.
x, y	Coordinates of the XY-stage

1. Introduction and motivation

Ambient light sensors are an inescapable factor in the modern world. Nearly every cellphone is equipped with one. The application in other devices like lamps or special equipment increases.

It is a challenge to manufacture colour sensors that are cheap and still accurate. An essential factor for the accuracy is the calibration of the sensors. A calibration process takes a lot of time. In production test a sensor has to be mounted onto a test platform, several light stimulus' have to be presented, each light stimulus has to be be measured by the sensor and a reference spectrometer, the sensors must be calibrated and finally the light stimulus have to be measured again to ensure proper calibration.

At this time colour sensors are calibrated by the customer and generally not by the manufacturer like *ams AG*. This shall be changed in the future so that calibrated sensors can be distributed. Calibrating this massive amount of sensors leads to great effort and costs. To improve the calibration process and lower the costs, two approaches can be taken into account. The first is to optimize the calibration process by itself. In other words the time for fixation, light situation simulation and measurements are reduced. The second approach is to calibrate multiple sensors simultaneously. That means that many sensors shall be calibrated at the same test site and with the same calibration spectrometer. For each additionally calibrated sensor at one site the average calibration time per sensor decreases. Many test sites and many expensive calibration spectrometers again would lead to higher costs, especially through maintenance.

This thesis is focused on high parallel optical testing and calibrating. The primary condition that must be fulfilled is that the sensor and the reference spectrometer sense exactly the same light condition. Depending on the type of sensor, colour, illuminance or both are measured. In this thesis particularly colour sensors are discussed and the calibration of illuminance is neglected.

To provide equal light conditions the initial approach is to just place more sensors under the calibration lamps. But as the number of sensors increases the light conditions will differ due to a lack of space. A diffuser plate promises more light homogeneity. But the far better diffuser is an integrating sphere. Due to it's nature all points on the sphere experience equal light conditions. Modifications of the sphere (port openings and numerous lamps) lead to a deterioration of this property. But with a sphere of sufficient size (1 m diameter in our case) and port openings that are small compared to the surface area the concept promises great light homogeneity for the calibration process.

The goal of this thesis is to test the approach with an integrating sphere to provide homogeneous light conditions for the high parallel sensor calibration.

2. Theory

The objective is to obtain a homogeneously lit surface. This section will go into the methods how the homogeneity is investigated. Shortly the relevant properties of integrating spheres are discussed. And finally the process of calibration is looked into.

2.1. Integrating sphere

Integrating spheres are widespread devices. Mostly they are used to measure the luminous flux of lamps. But there are also applications where a good angular homogeneity is needed. The use as homogeneously lit plane is rare. Most of those applications require only one lamp or several equal lamps. For the HPOT concept several different lamps have to be placed inside the sphere. A proper calibration requires at least three lamps, but a larger number is even better (see section 2.4). In our case up to 16 lamps are used (see section 3.2.2).

Even the best diffuser plate has a radial dependence of the scattered light. In an integrating sphere this is not the case and the points in the port plate should all experience the same light conditions. This is due to the way an integrating sphere works: "The projected solid angle from any point on a sphere to any element of area on the sphere is the same, regardless of location." [1, p. 67]. So in theory an integrating sphere provides perfect light homogeneity in a sphere segment. The perfect conditions are influenced by several factors:

1. The port plane is flat and therefore not a perfect sphere segment. Due to the large sphere radius this factor should be of minor effect. (The sagitta of the port plane and the integrating sphere is $\approx 16\,\mathrm{mm}$ for an integrating sphere with a $1\,\mathrm{m}$ diameter.)

2. Every port hole decreases the reflective surface. For the ports described in section 3.1 the integrating spheres surface is decreased by $\approx 2\,\%$.

3. Each baffle inside increases the reflective area and therefore improves the diffusive properties of the integrating sphere. The baffles described in section 3.1.2 increase the integrating spheres surface by $\approx 3\,\%$.

4. Since many lamps and equipment for fixation are placed inside the sphere the usual path for many rays is blocked. See section 3.2.1 for further details.

5. Each lamp is different and has a different light intensity distribution. In an empty sphere this theoretically wouldn't matter. In our case the various light intensity dis-

tributions behave very differently with the sphere interiors. Therefore experimental evaluation is necessary.

6. Every mirror, diffuser or integrating sphere has a leakage of luminous power. At first this doesn't matter since it will be about the same for all lamps. Secondly we are mainly interested in colour.

Taking point 2 and 3 into account the spheres surfaces only changes to 101 %. Therefore point 4 and 5 must have the mayor effect on the quality of the light diffusity. For further investigation a ray tracing program would be necessary. Still the theoretical approach to evaluate homogeneous plane illumination is very expensive in effort. This thesis only considers the experimental approach.

2.2. Tristimulus XYZ

Since colour is a value that depends largely on the perception of the human eye, it is not trivial to make it a measurable quantity. Through history there have been various attempts to define colour spaces that are practical for technical uses. The base for the most commonly used colour system is still one that was developed in 1931. At that time the International *Commission on Illumination* (CIE) defined the *CIE 1931 XYZ colour space*. The XYZ values are widely known as *Tristimulus*. They define a transformation from the electromagnetic visible spectrum to the colours perceived in human colour vision. Since humans generally don't perceive colours in exactly the same way, a standard observer is used. This has been achieved through numerous measurements with test persons. The values $\overline{x}(\lambda)$, $\overline{y}(\lambda)$ and $\overline{z}(\lambda)$ in the equations 2.1 are the CIE standard observer colour matching functions. $S_\lambda(\lambda)$ represents the spectral energy that shall be transformed to a point in the Tristimulus colour space. λ represents the electromagnetic wavelength over which is integrated in the range of human perceptibility (usually from 380 nm to 780 nm [1]).

$$\begin{aligned} X &= \int S_\lambda(\lambda) \cdot \overline{x}(\lambda) \cdot d\lambda \\ Y &= \int S_\lambda(\lambda) \cdot \overline{y}(\lambda) \cdot d\lambda \\ Z &= \int S_\lambda(\lambda) \cdot \overline{z}(\lambda) \cdot d\lambda \end{aligned} \tag{2.1}$$

The resulting values from the equations 2.1 represent the perception in long (X), middle (Y) and short wavelength regions (Z). The middle range colour matching function $\overline{y}(\lambda)$ also matches very closely the average spectral sensitivity of the human eye. Y therefore represents the luminance.

An illustration of the colour matching functions can be seen in figure 2.1. Data are only available in discrete values [1]. Due to the connection of $\overline{y}(\lambda)$ and the spectral sensitivity of the human eye, the colour matching functions are normalized to $\overline{y}_{max} = \overline{y}(555) = 1$.

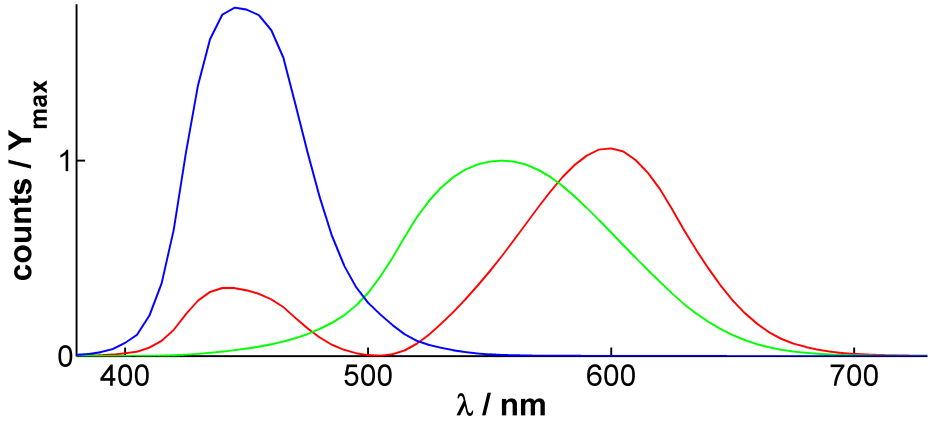

Figure 2.1.: The CIE standard observer colour matching functions for 2°. $\overline{x}$ represents long (red), $\overline{y}$ middle (green) and $\overline{z}$ short (blue) wavelength regions. The graphs are normalized to the maximal value of $\overline{y}$. [1]

2.3. Chromaticity difference

With the tristimulus values there is a defined measure for colour. But this gives even more information than is needed for our purpose. The information can be divided into lightness (illuminance) and chromaticity[1]. So when colour homogeneity is mentioned it always means chromaticity homogeneity in this thesis. To get rid of the unneeded degree of freedom the tristimulus values are normalized to the same illuminance value Y. Since the tristimulus colour space is linear it doesn't matter to which value Y is normalized. In the data evaluation of this thesis the tristimulus values are always normalized to $Y = 100$.

$$\begin{pmatrix} X \\ Y \\ Z \end{pmatrix}_{norm.} = \frac{100}{Y_{raw}} \cdot \begin{pmatrix} X \\ Y \\ Z \end{pmatrix}_{raw} \tag{2.2}$$

Colour perception and especially the perception of colour differences are very subjective. For the assessment of the colour homogeneity in the integrating sphere port plane two different methods are used. $\Delta_{u'v'}$ (see section 2.3.1) is wider spread in the technical sector. ΔE_{00} (see section 2.3.2) is better adapted to the human vision. In the end, both methods should show results which lead to the same conclusions.

2.3.1. Distance in the CIE (u'v') chromaticity diagram

The CIE (u'v') chromaticity diagram represents the uniform chromaticity space. The transformation from the tristimulus colour space is [6]:

$$u' = \frac{4X}{X + 15Y + 3Z} \qquad v' = \frac{9Y}{X + 15Y + 3Z} \tag{2.3}$$

[1] The chromaticity could further be divided into hue and saturation, which is not needed in our case.

A normalization of the tristimulus values wouldn't even be necessary for this transformation since the normalizing factors truncate.

The formula to get the chromaticity difference $\Delta_{u'v'}$ is simply the euclidean distance in the chromaticity plane [2, 6].

$$\Delta_{u'v'} = \sqrt{(u'_1 - u'_2)^2 + (v'_1 - v'_2)^2} \tag{2.4}$$

2.3.2. CIEDE2000 colour difference

On the contrary to $\Delta_{u'v'}$ the CIEDE2000 colour difference ΔE_{00} is capable of calculating colour differences in a three-dimensional colour space (so not only the chromaticity difference). Since we're only interested in chromaticity the mentioned normalization is carried out in advance.

ΔE_{00} is calculated in the CIELAB colour space. For the transformation a reference white (X_r, Y_r, Z_r) is needed. For this the CIE Standard Illuminant D65 with a 2° observer angle is chosen[2]. The transformation from the tristimulus colour space to CIELAB is:

$$x_r = \frac{X}{X_r} \qquad y_r = \frac{Y}{Y_r} \qquad z_r = \frac{Z}{Z_r} \tag{2.5}$$

$$f_t = \begin{cases} \sqrt[3]{t_r} & \text{if } t_r > \varepsilon \\ \frac{\kappa t_r + 16}{116} & \text{otherwise} \end{cases} \qquad \text{with } t \in \{x, y, z\} \tag{2.6}$$

$$\begin{aligned} \varepsilon &= 216/24389 \\ \kappa &= 24389/27 \end{aligned} \tag{2.7}$$

$$L = 116 f_y - 16 \qquad a = 500\,(f_x - f_y) \qquad b = 200\,(f_y - f_z) \tag{2.8}$$

The colour difference calculation in the CIELAB colour space has a long history with many attempts. $\triangle E_{00}$ is the most recent attempt, but also the most complex one. The algorithm is rather long and can be found in the appendix in section A.1.

2.4. Calibration

Due to the three different cone cells of the human eye, a colour is defined by three values (see section 2.2). In the case of the tristimulus the X, Y and Z values can represent all colours perceivable by the human eye. Colour information with more than three

[2] $(X, Y, Z) = (95.047, 100, 108.883)$ [1]

dimensions can still be mapped back to a three dimensional colour space without losing any information.

A colour sensor therefore needs at least three channels that cover different regions of the visible electromagnetic spectrum. In general those channels won't deliver calibrated data and the sensor needs to be calibrated. This is performed by a system of linear equations which are represented by a matrix multiplication. Equation 2.9 shows the easiest case where three channel values C_i are mapped to the tristimulus values XYZ.

$$\begin{pmatrix} X \\ Y \\ Z \end{pmatrix} = \begin{pmatrix} a_{11} & a_{12} & a_{13} \\ a_{21} & a_{22} & a_{23} \\ a_{31} & a_{32} & a_{33} \end{pmatrix}_{\mathrm{C}} \cdot \begin{pmatrix} C_1 \\ C_2 \\ C_3 \end{pmatrix} \tag{2.9}$$

Depending on the number of sensor channels n the calibration matrix $(a_{ij})_C$ has the dimensions $3 \times n$. Since it is hard to reproduce the cone sensitivity of the eye, many sensors compensate this weakness with additional channels.

2.4.1. Calibration matrix

To obtain the calibration matrix, measurements are performed with the sensor and a reference spectrometer at the same time. Of course each sensor gets it's own calibration matrix. But the reference spectrometer values can be used for parallel calibrations which is the substantive demand in this thesis.

The calibration matrix $(a_{ij})_C$ has $3n$ elements for n sensor channels. Therefore at least $m = n$ measurements with 3 colour coordinates are necessary to solve the system of linear equations. Equation 2.10 shows the matrix multiplication. Matrix $(X_j, Y_j, Z_j)_S$ with $j = \{1, ..., m\}$ represents the reference spectrometer measurements and matrix $(C_{kj})_D$ with $k = \{1, ..., n\}$ the uncalibrated sensor (DUT) measurements.

$$\begin{pmatrix} X_1 & \cdots & X_m \\ Y_1 & \cdots & Y_m \\ Z_1 & \cdots & Z_m \end{pmatrix}_{\mathrm{S}} = \begin{pmatrix} a_{11} & \cdots & a_{1n} \\ a_{21} & \cdots & a_{2n} \\ a_{31} & \cdots & a_{3n} \end{pmatrix}_{\mathrm{C}} \cdot \begin{pmatrix} C_{11} & \cdots & C_{1m} \\ \vdots & \ddots & \vdots \\ C_{n1} & \cdots & C_{nm} \end{pmatrix}_{D} \tag{2.10}$$

Generally this linear system is not solvable with analytical methods [5]. A numerical approach with the least squares method is performed. This however is no drawback, since a numerical approach is necessary due to another reason as well. With the mentioned linear system a sensor can be calibrated with m different measurements (m different lamps). For the sensor to be prepared for numerous light conditions a calibration with more lamps is desirable (see section 3.2). In our case up to 16 lamps are used.

The calibration works better when the illuminance (Y channel) is approximately the same for all measurements. It is expected that the reason for this can be found in the way the least squares method works. This was not investigated further and accepted as fact. To provide equal illuminance, dimmer packs were used instead of switches to control the lamps (see section 3.2.2). Unfortunately it was not easy to put this plan into effect. See section 4.2.1 for further details.

3. Experimental setup

To test if the high parallel optical test (HPOT) concept is possible, an integrating sphere is equipped with several different light sources. They are all mounted on a lamp-frame inside the sphere. Each of them can be switched and dimmed individually. The light then exits the sphere through a port at the bottom of the sphere. Under this exit port the colour sensors are placed for calibration. Through the equally illuminated area of the sphere many sensors can be illuminated at the same time. With the use of a spectrometer to provide reference values a calibration matrix for the sensors is obtained.

In production test many sensors will be calibrated at the same time. To test if the conditions are sufficient a spectrometer is used instead of a sensor. Subsequently one single sensor is used for proof of concept.

3.1. Integrating sphere

The integrating sphere was purchased from the company *Gigahertz-Optik*. It has a diameter of 1 m and weighs 32 kg. On the inside a barium sulfate coating is used which allows a high level of diffusion for the reflected visible light. The sphere consists of two hemispheres which can be screwed together. The top part is completely unmodified. The bottom part has three big holes for ports and four small holes to install the lamp-frame. In figure 3.1a the sphere is seen before assembling it onto the rack. Figure 3.1b shows the inside of the bottom hemisphere.

3.1.1. Sphere ports

The integrating sphere was equipped with three *Gigahertz-Optik* standard ports. In the middle of the bottom hemisphere is the light exit port with a 254 mm (10 inch) diameter. Next to the light exit port are two smaller ports with a 50.8 mm (2 inch) diameter. Their centres lie on a circle of 20 cm radius which is concentric to the light exit port. On this circle the two port centres lie 60° apart. All three ports have a notch where an adapter can be fixed with screws. The details can be seen in the figures B.2 and B.1 in the appendix.

Light exit port

When in use at the production test the sensors will be placed closely under this port. The original goal of the HPOT concept is to calibrate as many sensors simultaneously as possible. Therefore as many devices as possible must be placed under the light exit port simultaneously. For this number of devices there are two restricting factors. First the

(a) Integrating sphere before assembly onto the rack.

(b) The bottom hemisphere with the three ports.

Figure 3.1.: Integrating sphere before assembly (a) and bottom part (b).

quality of the homogeneously lit area that the integrating sphere can provide. Second the number of devices the chip-holder can carry. As discussed in the introduction (chapter 1) the first point is the major question that has to be answered in this thesis. The second factor is provided by the chip-holder that is planned to be used.

At the time the measurements were performed the most likeable choice could carry 256 devices. It is named *InCarrier* and manufactured by the company *Multitest*. A draft can be seen in figure 3.2. The whole testing process in the production is rather complex and an adaptation of the chip-holder just for the integrating sphere would lead to the necessity of many other adaptations and therefore a vast increase of costs. The fixation of the chip-holder on the testing system requires about 3 cm of space above. Therefore the devices are positioned 3 cm under the light exit port plain.

The designation of the light exit port is *UMPF-10.0*. It's exact dimensions can be seen in the appendix in figure B.2. In an early state of the project it was planned to make a diffuser plate attachable to this port. Since the integrating sphere itself should be the best possible diffuser and dust was considered to be a minor problem, the plan was discarded. A glass plate as protection against dust would have led to a different behaviour for different wavelengths of light and therefore was precluded too. The plans for a plate holder on the light exit port can be seen in the appendix in figure B.3.

Spectrometer port

The spectrometer probe which provides the reference measurements for the calibration must have the same light conditions like the sensors under the light exit port. Placing it in the middle of the light exit port would provide these light conditions. But it would also be very expensive in effort and costs to adapt the chip-holder accordingly. Besides that

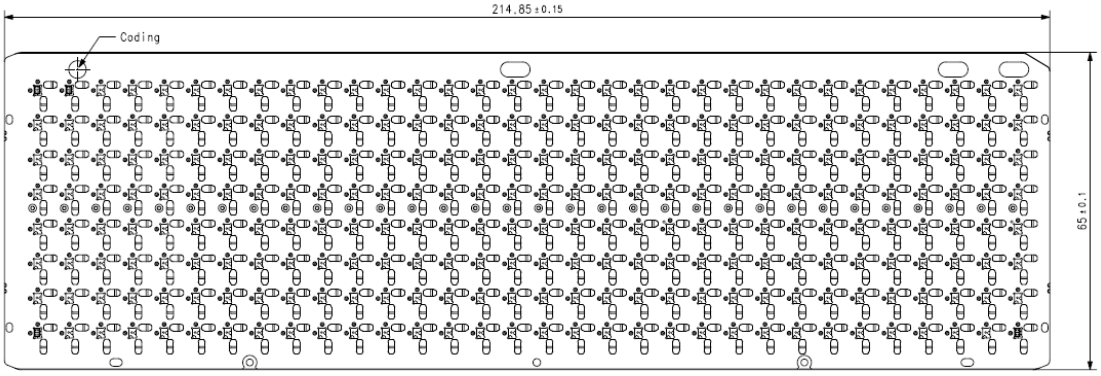

Figure 3.2.: *InCarrier* (chip-holder) of the company *Multitest*. 256 devices can be mounted and the diagonal measures about 225 mm.

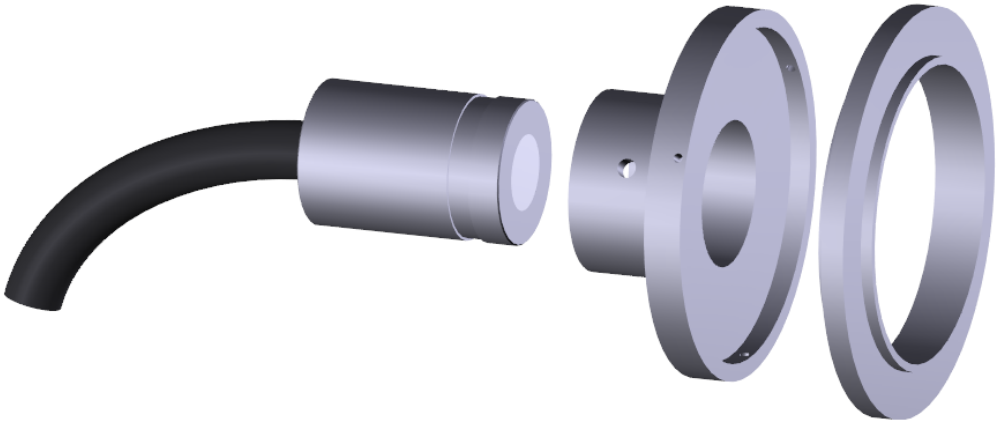

Figure 3.3.: The spectrometer probe with adapter and port.

there'd also be less space for sensors under the light exit port. The alternative attempt is to put the probe into a port right next to the light exit port.

The port used has the designation *UMPF-2.0*. It's exact dimensions can be seen in the appendix in figure B.1.

The spectrometer probe is attached to the port port with a specially designed adapter as seen in figure 3.3. The adapters exact dimensions can be seen in the appendix in figure B.4.

Cable port

All the lamps on the lamp-frame inside the sphere must be individually switchable. Therefore a small hole is not enough for the cables and another *UMPF-2.0* port is used. It's exact dimensions can be seen in the appendix in figure B.1. The port is not additionally sealed since the whole outer area is surrounded by an optically opaque

Figure 3.4.: Illustration of the lamp baffle around the socket.

curtain.

3.1.2. Baffles

Each surface inside the integrating sphere that is covered with the highly diffusive paint increases the diffusive properties of the sphere. So even though baffles cast shadows, they also increase the diffusive area.

Lamp baffles

Using integrating spheres the light must never shine directly into a detector. Using 16 lamps, there have to be 16 baffles as well. The easiest way, that also shields the least area of the lamp, is to mount the baffles around the sockets. Since the lamps are tilted and must shield a circular region (the light exit port) an elliptical shape was chosen. An illustration can be seen in figure 3.4.

Port baffle

The light exit port takes away a rather large area of the sphere. To counteract this decrease of diffusive area the port is covered with a movable baffle. This simulates the reflective area of the chip-holder while allowing the spectrometer probe to move. The port baffle is circular with the diameter of the light exit port as radius. In the middle is a hole for the spectrometer probe or a sensor. The whole baffle is fixed on a pole which is mounted on the XY-stage. Thus measurements in the whole port plain can be conducted while the rest of the port is sealed with the baffle. This simulates An illustration of the port baffle can be seen in figure 3.5.

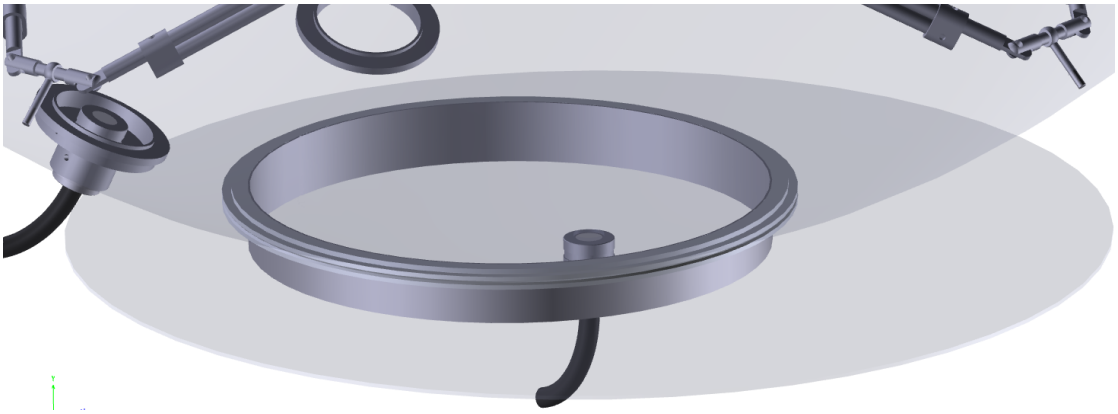

Figure 3.5.: Illustration of the port baffle.

It was tested that through the port baffle the measured light intensity increases by about 20 %. The lamp, the dim level and all other parameters remained the same.

The arising gap between the port and the chip-holder is covered with a 3 cm long tube. It is also coated with the diffusive paint.

3.1.3. Rack

For a convenient accessibility the sphere is mounted on a rack designed by the company *Haberkorn*. It can be seen in figure 3.6. The rack makes it easily possible to open the sphere and perform adjustments inside. Besides that there needs to be enough space under the sphere for the XY-stage and the spectrometer probe. The probe is rather small. But the optical fibre leading from the spectrometer to it's probe must not be bent to a smaller radius than 22 cm.

The top half of the sphere is separated from the bottom half by a hinge and lifted by two gas springs. For security reasons it is then fixed by a snap-in latch.

Originally the sphere is not designed to be opened like this. The design planned to screw the two halves together and only separate them rarely. However, since it is necessary to open the sphere rather frequently, the hemispheres are not screwed together. The bottom hemisphere is fixed to the still part of the rack, respectively the top hemisphere to the hinged part. Unfortunately the rack and the hinges are not very precise. So the two hemispheres aren't perfectly flush mounted. For the screws countersunk heads are used. Unfortunately the second hole of each of the eight corners aren't accessible due to the design. The construction leads to a gap of 0 to 2 mm between the two hemispheres. This may seem unpleasant, but turned out to have minor effects. Measurements didn't change due to this small light leakage in a notable range, no matter if the room lights were turned on or off.

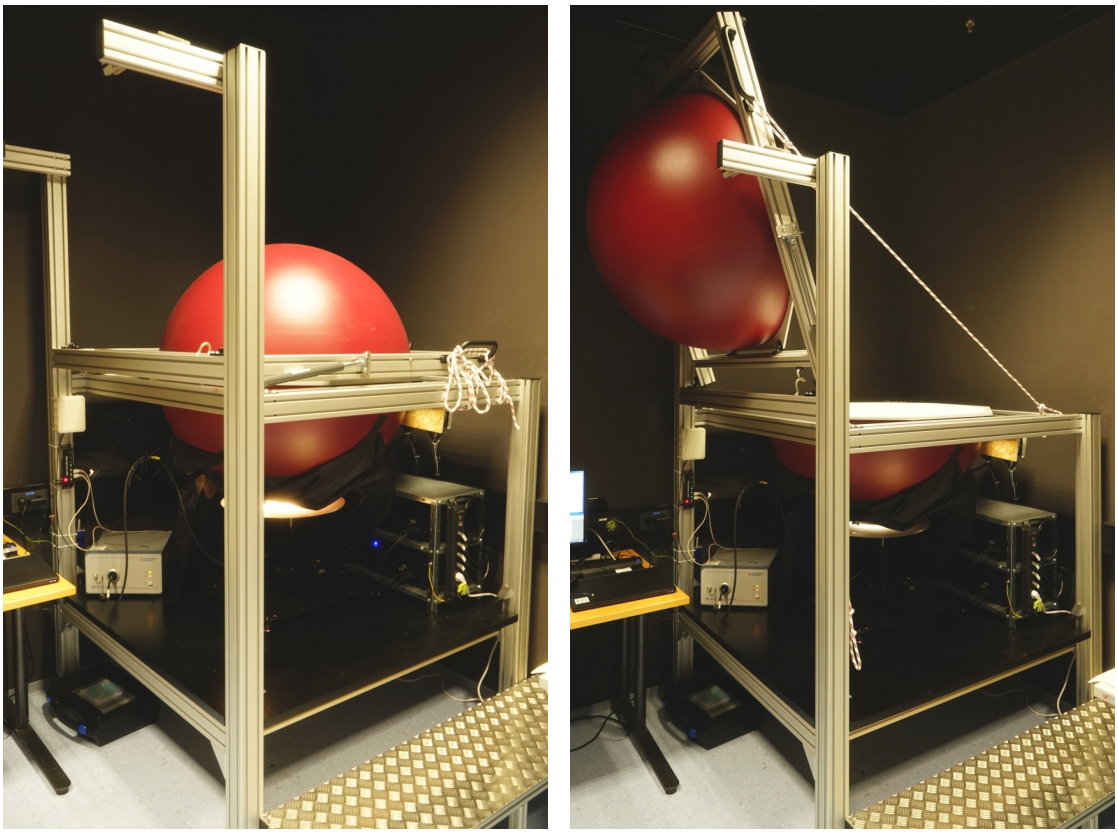

Figure 3.6.: Integrating sphere inside the rack in closed (left) and opened (right) state.

3.2. Lamps

The ambient light sensors, that will be calibrated using the HPOT concept, must be capable to function with many different light situations. The focus lies on most likeable light situations like sunlight and room light with different lamp types. All of them are white with a varying colour temperature.

Since two lamp types with the same colour temperature generally don't emit the same electromagnetic spectrum the use of different lamp types is very important. For instance will a sensor detect a 4000 K LED very differently than a 4000 K fluorescent lamp.

Table 3.1 shows the selection of lamps which have been chosen for the project. 16 of them can be placed in the lamp-frame simultaneously.

3.2.1. Lamp-frame

A lamp inside an integrating sphere is best placed right in the middle. Since there are 16 lamps used simultaneously in this project, the arrangement isn't that simple. Especially because non of the lamps must shine directly onto the light exit port or the spectrometer port. As mentioned in section 3.1 the integrating sphere provides four small holes to install the lamp-frame.

The lamp-frame is mostly made of matted aluminium parts. The light exit port is a circular slat with about 60 cm in diameter. There are four joint-sledges on it which connect the frame to the sphere with eight poles. Each joint-sledge is connected to two different sphere holes, which ensures stability through triangles. The lamps are attached to the frame with another movable sledge, which can tilt the lamp socket. Pictures of the lamp-frame can be seen in figures 3.7 and 3.8. Since the diameter of the frame, the pole lengths and the lamp tilting all can be changed, the lamp-frame provides a lot of flexibility.

Ideally everything inside the sphere should be painted white. But since most parts would scrape off paint, when they are moved, only the parts directly at the lamp sockets are painted.

In the end, the parameters of the lamp-frame weren't changed a lot. To find the ideal position for the lamps a lot of trial and error or a ray tracing program would have been necessary.

3.2.2. Dimmerpacks

To switch and dim the lamps four *Eurolite EDX-4R DMX RDM Dimmerpacks* are used. All four again control four channels each. Hence 16 lamps can be addressed individually.

Using a computer the dimmerpacks are controlled by a USB-to-DMX-interface called *Enttec Open DMX USB*. Each dimmerpack has a DMX-In and a DMX-Out port. Thus they can be run in a series connection. The DMX-Out port of the last dimmerpack needs an end resistor so that the DMX protocol works appropriately.

The start channel of each dimmerpack can be set manually. Therefore the 16 channels can be addressed from 1 to 16. The channel values (dimming values) go from 0 to 255.

Table 3.1.: Selection of lamps chosen for the project.

Type . . . . Type of the lamp used (Fluorescent, LED or Incandescent).
Brand . . . Manufacturer
CCT . . . . Correlated colour temperature in K. (As stated on the packaging.)
P . . . . . Consumed power in W. (As stated on the packaging.)
LO . . . . . Light output in lm. (As stated on the packaging.)
Dim . . . . . States if the lamp is dimmable.
Label. . . . Names the lamp in this thesis. (Type - CCT - Light output)

Type	Brand	CCT	P	LO	Dim	Label
		K	W	lm		
Fluorescent	Philips	2700	20	1220	✓	ES1-2700-1220
Fluorescent	Osram	4000	7	430	✗	ES2-4000-430
Fluorescent	Osram	4000	8	430	✗	ES3-4000-430
Fluorescent	Osram	4000	14	740	✗	ES4-4000-740
Fluorescent	Osram	4000	18	1140	✗	ES6-4000-1140
Fluorescent	Osram	6500	7	400	✗	ES7-6500-400
Fluorescent	Osram	6500	14	730	✗	ES8-6500-730
Fluorescent	Megaman	6500	14	810	✗	ES9-6500-810
Fluorescent	Megaman	6500	20	1215	✗	ES10-6500-1215
LED	Osram	2700	10	806	✓	LED1-2700-806
LED	Sylvania	3000	8	500	✓	LED2-3000-500
LED	Osram	4000	9	806	✓	LED3-4000-806
LED	Renkforce	5900	6	430	✓	LED4-5900-430
LED	Sygonix	6500	7	550	✓	LED5-6500-550
LED	Paulmann	6500	10	806	✓	LED6-6500-806
LED	Mlight	6500	11	1100	✗	LED7-6500-1100
Incandescent	Osram	2700	30	405	✓	H1-2700-405
Incandescent	Osram	2700	46	700	✓	H2-2700-700
Incandescent	Sygonix	2800	52	778	✓	H3-2800-778
Incandescent	Osram	2800	77	1320	✓	H4-2800-1320

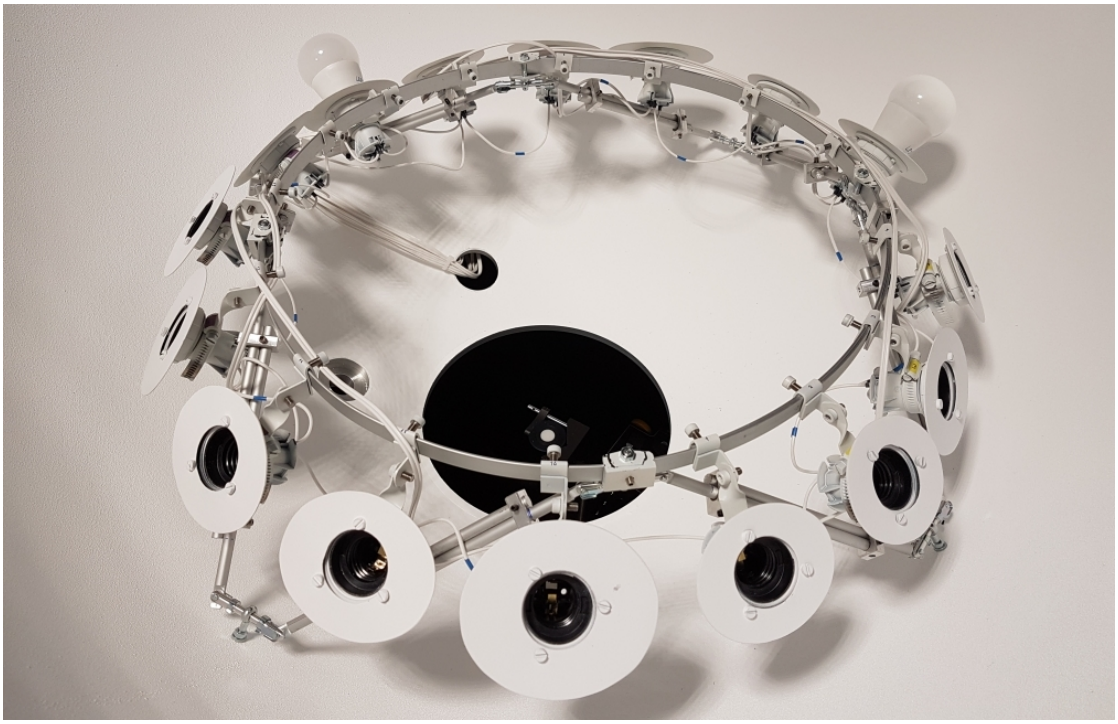

Figure 3.7.: Lamp-frame. In the middle of the light exit port the spectrometer probe can be seen.

Figure 3.8.: Lamp-frame with lamps, before the lamp baffles were attached.

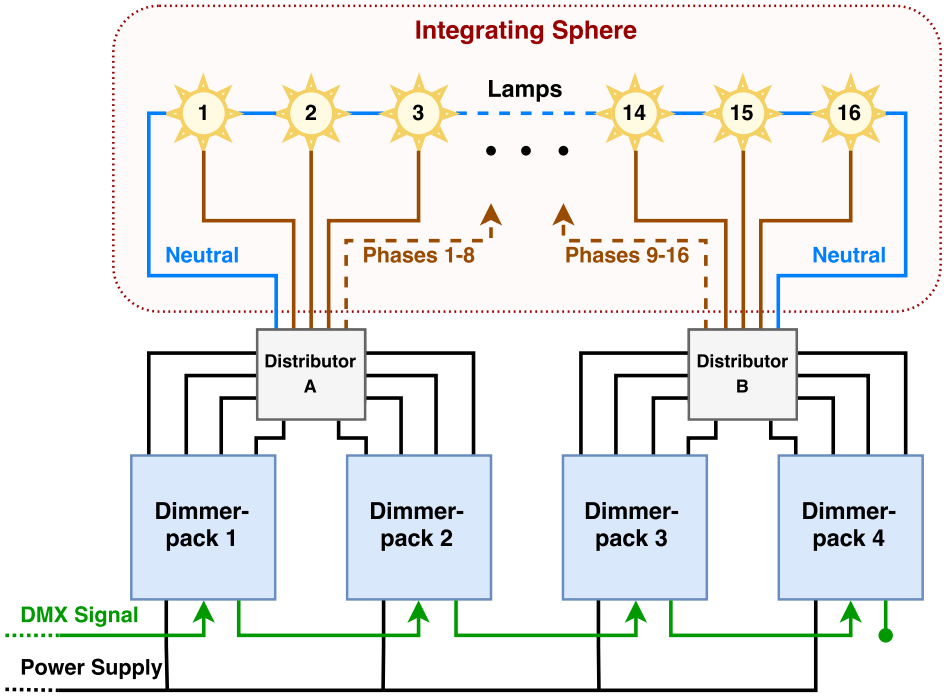

Figure 3.9.: Circuit diagram of the lighting system.

If a value is set to 0 the corresponding lamp is completely switched off. The channel number and the dimming value are the only two values that need to be sent to the USB-to-DMX-interface by the software used.

The dimmerpacks provide conventional power plugs for the lamps. To minimize the amount of cables that have to enter the integrating sphere the phase-cables were extracted from the cable bundle and the neutral-cables were combined to two cables. Only one would be necessary, the second is backup. The circuit diagram with the dimmerpacks and lamps is illustrated in figure 3.9.

3.3. XY-stage

Two *Thorlabs LTS300* linear translation stages are combined to a XY-stage. On the sledge a pole is mounted with the spectrometer probe on top. In this way the probe can be moved to different positions under the light exit port. Each stage can be positioned between 0 and 300 mm. The inaccuracy is less than 47.0 µm and therefore by far accurate enough [9].

Both stages are connected to the computer by an USB-cable. For the experiment only the X- and Y-coordinates are important. With the software (see section 3.6) also the acceleration and the velocity of the sledges can be set. For a convenient use the centre position of the light exit port is defined as point of origin. Thus this point can be handled

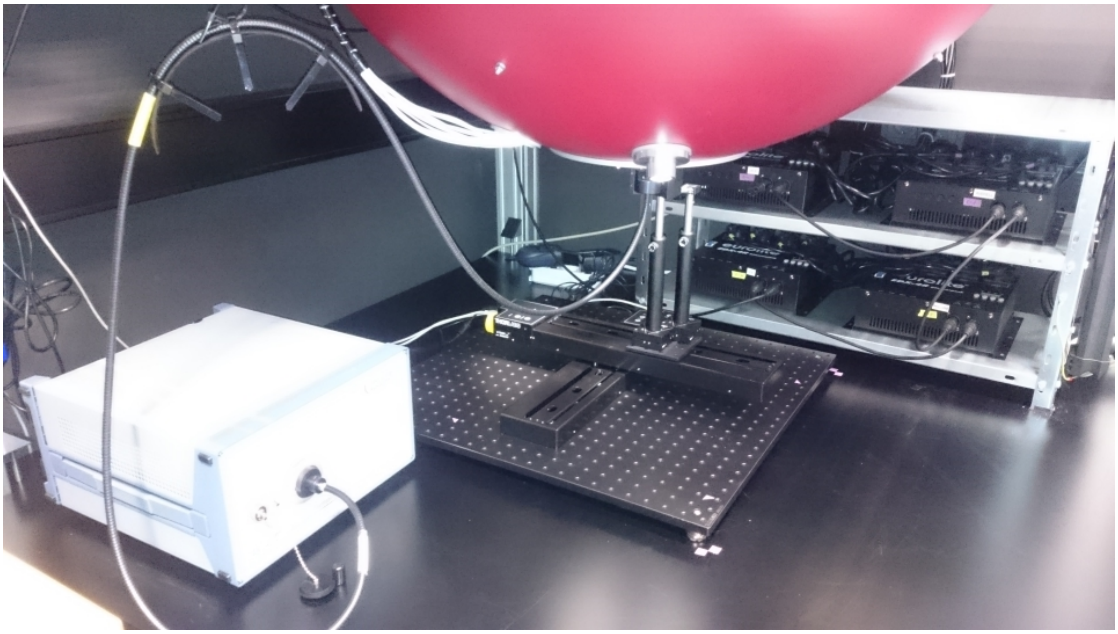

Figure 3.10.: XY-stage with the spectrometer probe. The spectrometer is on the left with the fibre cable leading to the probe. At the back on the right the dimmers can be seen.

by the software as (0,0) even though it would actually be something like (150,150).

A picture of the XY-stage with the spectrometer probe can be seen in figure 3.10.

3.4. Spectrometer

The *CAS 140CT* spectrometer is the main measurement device for this project. It is manufactured by the company *Instrument Systems*. One application is to provide reference measurements for sensor calibrations. Another one is to examine the homogeneous light conditions of the light exit port plain. In production test also this type of spectrometer will be used.

The spectrometer is accepted in the industry as high end instrument. It provides a spectral resolution of down to 3.7 nm in the range from 300 nm to 1100 nm [4].

For some sensors not only the colour point, but also the illuminance has to be measured for calibration. Most spectrometers are built to map the relations of the spectral intensities as accurately as possible. The absolute illuminances on the other side are not their strength. In this thesis however, only the colour calibration is discussed and the absolute illuminance is subsidiary.

The spectrometer measures the spectral response (counts) for the whole defined wavelength area (which is normally the sensitive range). Combining them with the standard observer functions the tristimulus values X, Y and Z are calculated (see section 2.2). This is performed in a way that the Y-channel represents the total illuminance. With the tristimulus

values all colours perceptible by the average human eye can be represented.

The spectrometer probe used is called *EOP-09146*. It's entrance is covered with a circular diffuser of 1 cm in diameter. Through the diffuser the probe has a cosine-sensitivity obeying Lambert's cosine law approximately [4]. The cosine-sensitivity is nice to have, however it isn't essential because the integrating sphere itself provides a behaviour like that. An illustration of the spectrometer probe can be seen in figure 3.3.

3.5. Device under test (DUT)

In general a colour sensor needs to have at least three channels that the signals can be transformed to tristimulus values. More channels can lead to a more accurate result. Especially when their spectral sensitivity lies in a wavelength region that is characteristic for certain lamp types. For example slightly longer wavelength regions than the visible light can be useful to sense incandescent lamps.

The colour sensor that is used to test the HPOT concept has four channels. Three that are imitating the tristimulus channels (X, Y and Z) and one in the near infrared region (IR). Various values can be set for operating the sensor. Three of them are stated here without further explanation but for reproducibility:

1. Integration time: 78 ms
2. Gain: 16x
3. Averaging number: default

Their variation shouldn't change the sensed colour but might increase the accuracy.

3.6. Software

Since controlling all the components manually would be a lot of effort, a software is used for that. It was designed particularly for this measurement setup and can control:

1. the XY-stage,
2. the dimmerpacks,
3. the spectrometer
4. and the device under test (DUT).

Unfortunately only the integration of 1 to 3 was finished until the measurements were executed.

In principle the software sends parameters to all devices and receives measurement data from the spectrometer and the DUT. A diagram for easy understanding can be seen in figure 3.11. The software is not performing any calculations. The measured data are saved in csv-files and the evaluation is performed with Matlab and Excel.

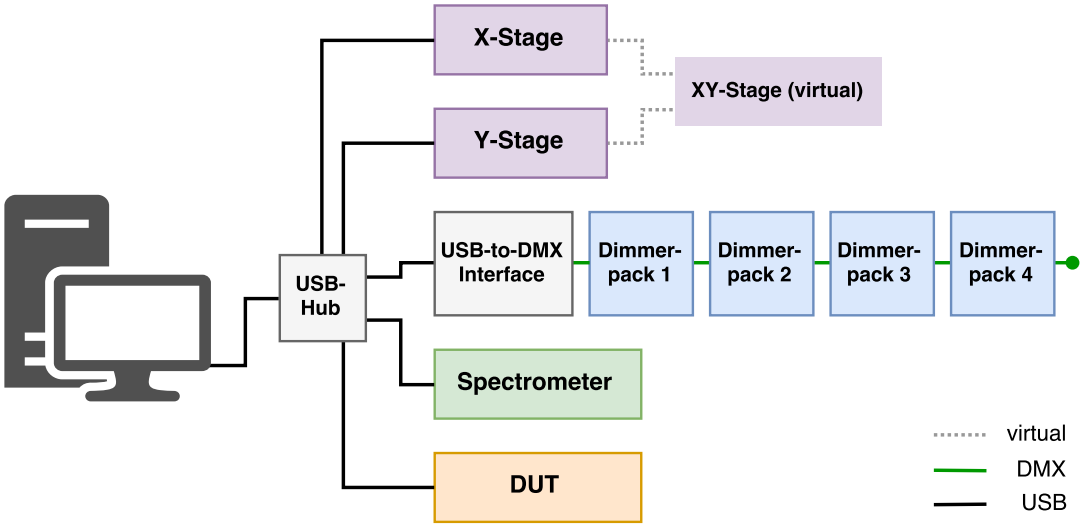

Figure 3.11.: Software diagram showing how the devices used are connected.

The details for controlling the devices are rather complicated. Since they are not important for the project and would go beyond the scope of this thesis they are not further investigated. Instead the essential functions used are explained.

3.6.1. Lamp setups

To ease the call of the functions of this software, lamp setups were defined. They are a list of all 16 lamp channels with a corresponding dimming level for each channel. Besides that a "switch on time" in milliseconds is listed. It states the time a group of lamps needs to be switched on. This is not to confuse with the time they need to come to full luminous power.

The lamp setups can be called by the functions only by their name. Even though this section always mentions "lamp setups" eventually they are only single lamps. But through this approach it would be easily possible to use two lamps instead of one, if for instance one lamp would be too weak. Table 3.2 shows how a lamp setup file is structured.

3.6.2. Functions

There are two main reasons for the automation. Firstly many single measurements have to be done for a homogeneity measurement of reasonable grid size. Secondly for a HPOT measurement the individual DUT and spectrometer measurements have to be taken shortly after each. Besides that, mistakes because of oversight can be minimized.

In the end, an XY- or HPOT measurement can be performed only by calling the corresponding command right after calling the command for performing a dark current

Table 3.2.: Example lamp setup table. The values entered are arbitrary and not the ones that are used.

LSN . . . . . Lamp setup name
Ch1-16 . . . Dimming values of the channel
SOT . . . . . Switch on time in ms

LSN	Ch1	Ch2	...	Ch16	SOT
LS1	255	0	...	0	2000
LS2	0	210	...	0	500
...	...	...	...	...	...
LS16	0	0	...	220	1000

measurement. The parameters for the spectrometer are stored in an options file and are the same for all measurements.

Dark current measurement

Like mentioned in section 3.4 a dark current measurement has to be taken periodically. The spectrometer then subtracts the dark current spectrum automatically and it doesn't have to be considered by the other functions. In general a DC measurement should be taken before every measurement series. Under normal conditions it can be considered valid for at least half an hour, but probably even longer. This is absolutely sufficient for our usage.

XY-grid measurement

This function performs the homogeneity measurements. Subsequently different coordinates under the light exit port are steered to and a spectrometer measurement is performed for each point. The coordinates are passed to the function with a coordinates file. The file just contains a two-columned table of x- and y-coordinates. Besides the coordinates also a lamp setup name is passed to the function. On executing the command the desired lamp setup is switched on and its "full illuminance time" is waited before performing the homogeneity measurements. That is because the light conditions inside the sphere shouldn't change while measuring different coordinates. After measuring the data for the last coordinate in the list, the coordinates and the corresponding tristimulus values are saved in a csv-file. They can then later be further processed by Matlab and Excel to obtain a homogeneity pattern. An example for the output file can be seen in table 3.3.

HPOT measurement

The purpose of this function is to obtain the data that are needed to calibrate a sensor. The measurement is only performed by one sensor even though the function is called "HPOT".

Table 3.3.: Example output of the XY-grid measurement function. The entered values are arbitrary.

x, y ..... XY-stage coordinates
X, Y, Z ... Tristimulus

x	y	X	Y	Z
0	0	1000	900	1100
0	10	1010	905	1080
...	...	...	...	...

Table 3.4.: Example output of the HPOT measurement function. The entered values are arbitrary.

LSN ..... Lamp setup name
X, Y, Z ..... Spectrometer tristimulus
X-, Y-, Z-, IR_DUT ... Channel counts of the DUT

LSN	X	Y	Z	X_DUT	Y_DUT	Z_DUT	IR_DUT
LS_1	1000	900	1100	500	450	550	700
LS_2	1200	1000	1100	600	500	550	100
...	...	...	...	...	...	...	...

The input parameter for this function is a list of lamp setup names. Those lamp setups are then successively switched on. For each one of them both, a spectrometer and a DUT measurement are performed. After the last lamp setup was measured the resulting data are stored in a csv-file which then can be further processed to obtain a calibration matrix of the sensor used.

The output file contains a list of lamp setup names, the tristimulus values measured by the spectrometer respectively the channel values measured by the DUT. An example can be seen in table 3.4.

Lamp setup calibration

The calibration of a sensor works best, when the lamps used shine with about the same luminous power. These functions aim is to get the dimming values for the desired lamp setups in a way that they all shine with approximately the same luminous power. Since this is generally not the case, it must be tested. The process to do so requires the following steps after an obligatory dark current measurement:

1. A dimming curve is measured for each lamp setup. That means that the setup is switched on with the full dimming level of 255. The "full illuminance time" is waited. Then the dimming level is reduced every 500 ms by one digit. A spectrometer measurement is taken for each step.

2. The illuminance for the full performance (dimming level of 255) is compared for each dimming curve. The lamp setup with the lowest value is the reference lamp setup to which the others have to be adapted. It's maximal value is the reference illuminance.

3. Then the dimming value with the lowest illuminance difference to the reference illuminance is searched for each lamp setup. The corresponding dimming values are saved to a new lamp setup list. As a result a lamp setup list with setups of minimal luminous power differences is obtained.

In theory this all may seem reasonable and target-aimed. Unfortunately it doesn't work that easily. The problems are discussed in section 4.2.1.

4. Measurement procedures

For good light conditions the spectrometer probe is fitted into the spectrometer port right next to the light exit port (see section 3.1.1). Besides providing the reference measurements for sensor calibration, the spectrometer is also used to measure the colour homogeneity in the light exit port plain. This is conducted through mounting the spectrometer probe on the XY-stage (see section 3.3) and moving it in the port plain.

To eliminate stray light from the outside a curtain was installed between the integrating sphere and the measurement table. In combination with the port baffle (see section 3.1.2) this led to very good sealing of the exterior light. Even though the light in the optical lab didn't influence the measurements in a noticeable way it was always switched off.

Since the port baffle was installed after the curtain not much space was planned inside. It was sufficient when the XY-stage is concealed. Since the port baffle has a radius of the light exit port diameter a lot more space was needed. Fortunately there was still sufficient space. But the XY-stage shouldn't be moved to other positions than those right under the port or the home position (see section 3.3). Especially for the DUT calibration measurements it has to be taken care of the XY-stages position. When the spectrometer probe is fitted into the probe port the port baffle could bump into the probes fibre and damage it.

To provide enough flexibility for the optical fibre of the spectrometer in the various situations, it was hung up on a rail that supports it's limited bending radius. An illustration can be seen in figure 3.10.

4.1. Colour homogeneity

The last step before performing a colour homogeneity measurement is to define coordinates. The middle of the light exit port is defined as point of origin $(0, 0)$. For convenience a reticle was put onto the port and the XY-stage was moved to the point of intersection. The coordinates (e.g. $(148, 153)$ in millimetres) are saved in the options file of the measurement program and are from now on addressed as $(0, 0)$. It shall be mentioned that the XY-stage operates in millimetres, but the evaluation is done in centimetres.

At the point of origin the dark current measurement is performed. Afterwards the first measurement starts right there. Successively the other points are approached and a measurement is taken for each one. The order can in principle be arbitrary but the same grid was used for all measurements. It's coordinates can be seen in the appendix in table B.1.

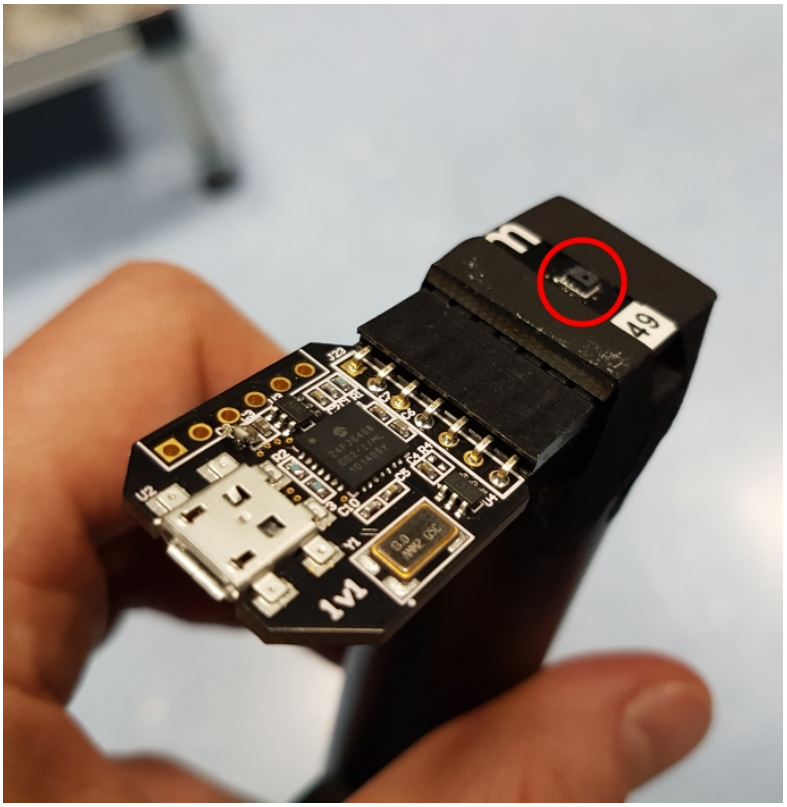

Figure 4.1.: Sensor fixed on the mounting. The red circle highlights the sensor.

4.2. DUT calibration

Like mentioned earlier in this section when the spectrometer probe is placed in the probe port it has to be taken care that the fibre is not damaged by the port baffle.

For the fixation of the sensor a 3D-printed bracket was designed. Unfortunately the sensor is not centred well in the aperture (port baffle) when mounted in this bracket. Therefore it was attached on a rod with tape which was fastened by the same clamp that also holds the spectrometer probe when fitted on the XY-stage. A picture can be seen in figure 4.1.

After positioning the sensor and the spectrometer, successively the lights have to be switched on and measurements have to be taken. This must happen as simultaneously as possible with both devices. Originally the software automation must ensure a minimal delay. But since this part of the software wasn't finished timely, the measurements were taken manually. This may have caused delays between 0 and 0.5 s. With constant lighting this wouldn't matter. But since the measurements are taken shortly after switching on the lamps, constant lighting is not the case. Every lamp and especially lamp type performs differently on start-up.

4.2.1. The dimming problem

As mentioned in section 2.4 the calibration process achieves better results when the lamps are dimmed to equal luminous power (equal illuminance (Y channel) is measured). It cannot be taken for granted that a lamp behaves linearly or even consistently when dimmed. Neither would be necessary to obtain appropriate dimming values. The problem is, that the lamps behave very unpredictable when they are switched on. So in the first place the approach with the "lamp setup calibration" function (see 3.6.2) isn't the appropriate choice. The reason is that the lamps at first are fully illuminated and then dimmed. This can't be done in production test, since it requires too much time.

The approach in the different direction, to switch on the lamps for a certain time and with a certain dimming level isn't promising either. Since the switch-on behaviour is rather unpredictable with full dimming level, it is likely to be even more complicated when a lamp is switched on to a dimmed level. Due to those difficulties the measurement time window for equal illuminance would be very small.

In production test measurement times will be short and it is not possible to wait until a lamp has reached full illumination. Besides the dimming and the switch-on problems, several other factors like the lamp temperature also change the lamp characteristic. In the end, dimming lamps that need several seconds before reaching usable brightness levels isn't reasonable.

The fact remains that equal illuminance for each measurement is worth striving for. In chapter 7 possibilities are discussed that could lead to more success.

5. Results

We looked at two ways of calculating the colour difference: ΔE_{00} and $\Delta_{u'v'}$. Both values are roughly equivalent and allow the same conclusions to be made. For completeness all plots are shown with both methods.

The colour differences are acceptable when $\Delta E_{00} < 1.5$ and $\Delta_{u'v'} < 0.002$ respectively. This means that two colours are perceived to be the same by the human eye. For legibility $\Delta_{u'v'}$ is multiplied by 10^3. The criterion is therefore $\Delta_{u'v'} \cdot 10^3 < 2$.

5.1. Colour homogeneity

For the evaluation of the colour homogeneity in the light exit port plain, measurements with each of the three lamp types are investigated. The figures 5.1 to 5.6 show a view of the whole light exit port as a circle with each measured value at the specific coordinate. The data point outside of the circle is the probe port. The reference value for the colour difference is always the one measured at the probe port.

Even though these plots already look very promising we want to tidy the information. The figures 5.7 to 5.12 show the colour difference mapped to the distance from the probe port d_{port}. The uncertainty handling is described in chapter 6.

5.2. DUT calibration

The DUT calibration was performed as explained in section 4.2. Figure 5.13 and 5.14 show the colour difference between the calibrated DUT and the spectrometer. A full lamp-frame with 16 lamps was used to calibrate the DUT. Since the values were not very satisfactory a different selection of lamps was tried. Figure 5.15 and 5.16 show the results of the smaller selection of lamps. Table 5.1 indicates which lamps were used for which measurements.

As a very experimental attempt it was tried to use the correlated colour temperature (CCT) of a colour point as a fourth calibration value besides the tristimulus. The results can be seen in figure 5.17 and 5.18. It must be mentioned that this only makes sense when the DUT channel sensitivities imitate the cone cells of the human eye. Even though this attempt was a random shot, it led to slightly improved results, especially for incandescent lamps.

Table 5.1.: Selection of lamps chosen for the measurements.

Type ... Type of the lamp used (Fluorescent, LED or Incandescent).
CCT ... Correlated colour temperature in K. (As stated on the packaging.)
LO ... Light output in lm. (As stated on the packaging.)
Label ... Names the lamp in this thesis. (Type - CCT - Light output)
Full ... Indicates which lamps were used in the full lamp frame.
Sel. ... Indicates which lamps were used for the smaller selection.

Type	CCT	LO	Label	Full	Sel.
	K	lm			
Fluorescent	2700	1220	ES1-2700-1220	✓	✓
Fluorescent	4000	430	ES2-4000-430		
Fluorescent	4000	430	ES3-4000-430	✓	
Fluorescent	4000	740	ES4-4000-740	✓	
Fluorescent	4000	1140	ES6-4000-1140	✓	✓
Fluorescent	6500	400	ES7-6500-400	✓	✓
Fluorescent	6500	730	ES8-6500-730	✓	✓
Fluorescent	6500	810	ES9-6500-810	✓	✓
Fluorescent	6500	1215	ES10-6500-1215	✓	
LED	2700	806	LED1-2700-806	✓	
LED	3000	500	LED2-3000-500	✓	✓
LED	4000	806	LED3-4000-806	✓	✓
LED	5900	430	LED4-5900-430	✓	
LED	6500	550	LED5-6500-550		
LED	6500	806	LED6-6500-806		
LED	6500	1100	LED7-6500-1100	✓	✓
Incandescent	2700	405	H1-2700-405		
Incandescent	2700	700	H2-2700-700	✓	✓
Incandescent	2800	778	H3-2800-778	✓	✓
Incandescent	2800	1320	H4-2800-1320	✓	✓

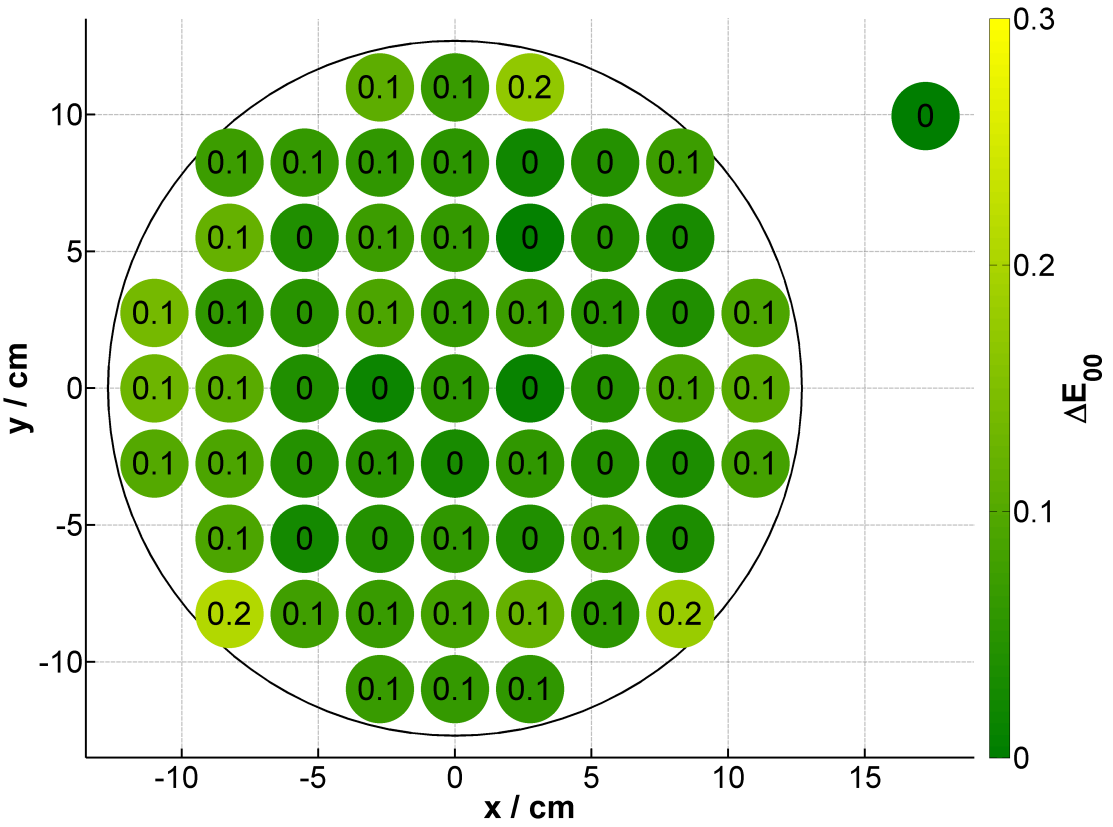

Figure 5.1.: Homogeneity measurement using a 4000 K fluorescent lamp (ES4-4000-740). The data points represent the colour difference ΔE_{00} to the probe port.

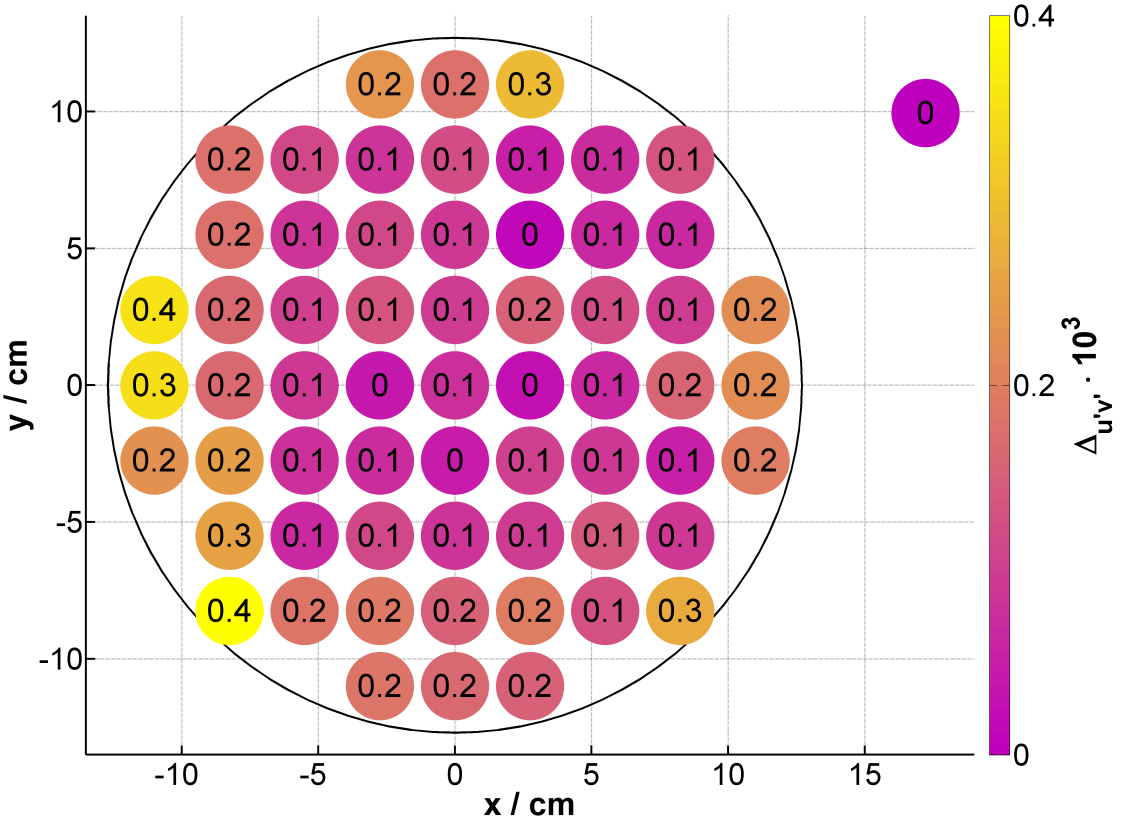

Figure 5.2.: Homogeneity measurement with a 4000 K fluorescent lamp (ES4-4000-740). The data points represent the colour difference $\Delta_{u'v'} \cdot 10^3$ to the probe port.

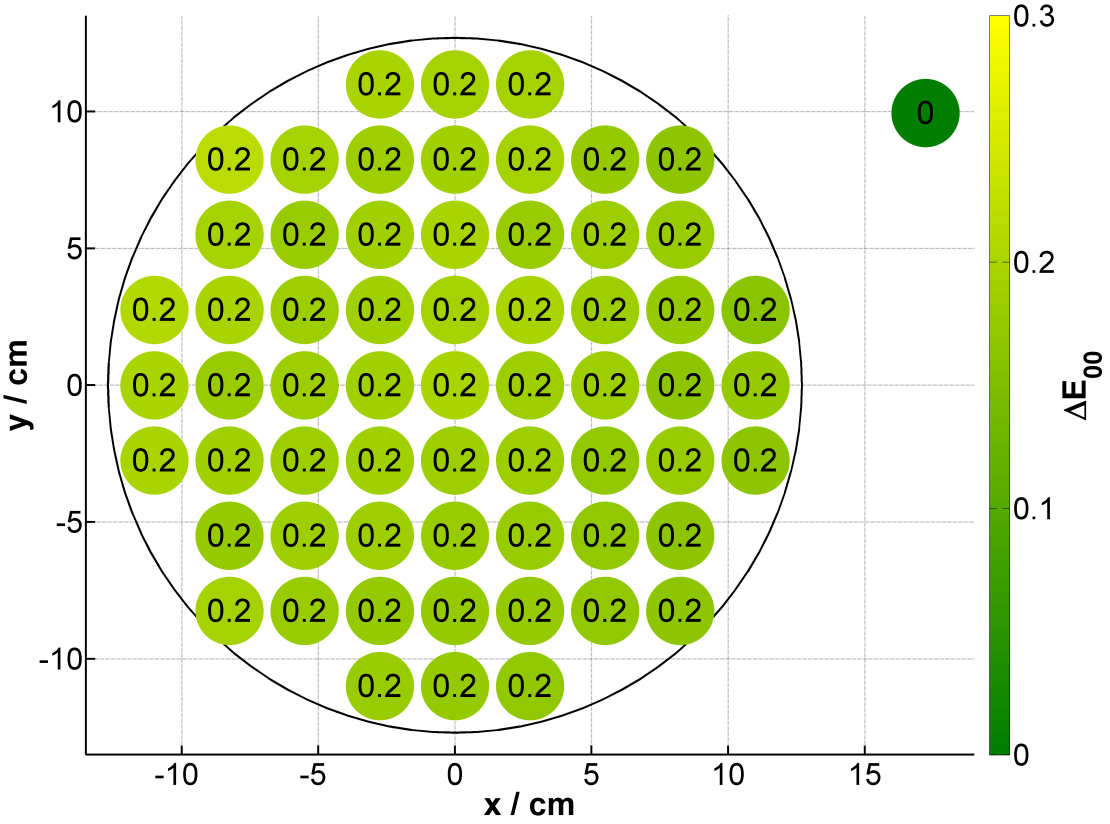

Figure 5.3.: Homogeneity measurement with a 2700 K LED lamp (LED1-2700-806). The data points represent the colour difference ΔE_{00} to the probe port.

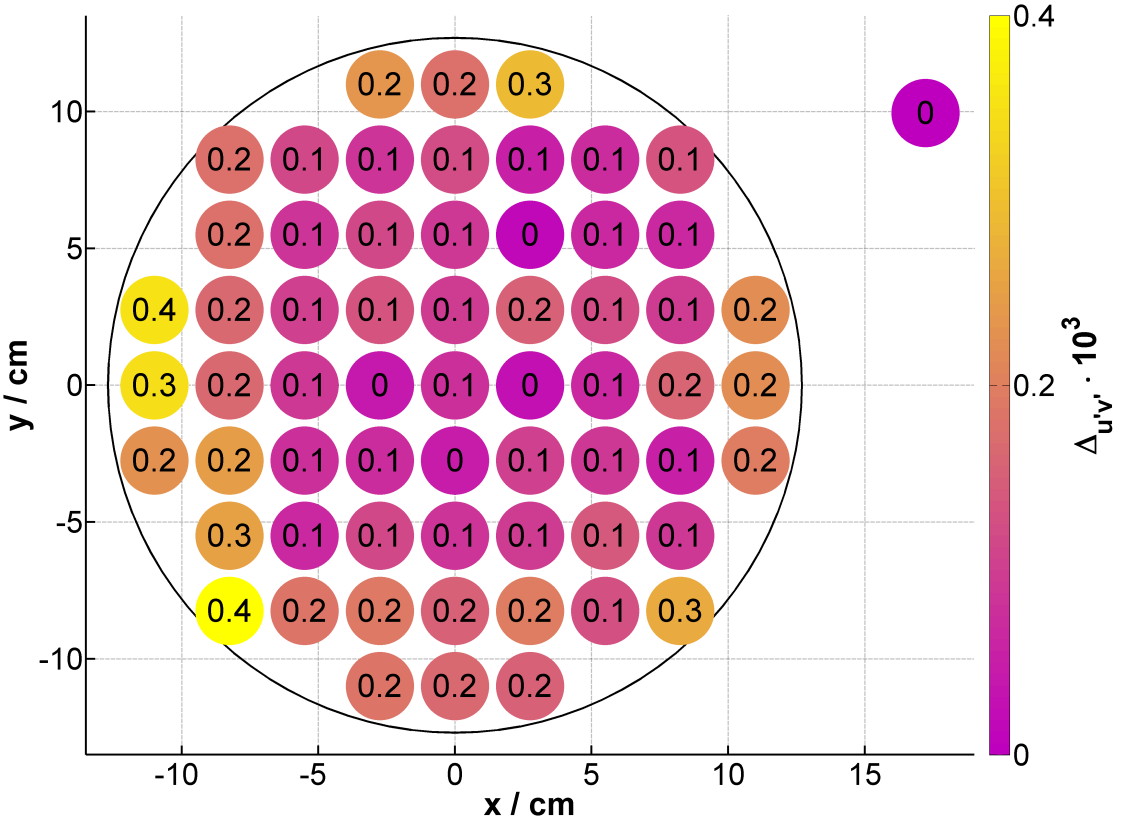

Figure 5.4.: Homogeneity measurement with a 2700 K LED lamp (LED1-2700-806). The data points represent the colour difference $\Delta_{u'v'}$ to the probe port.

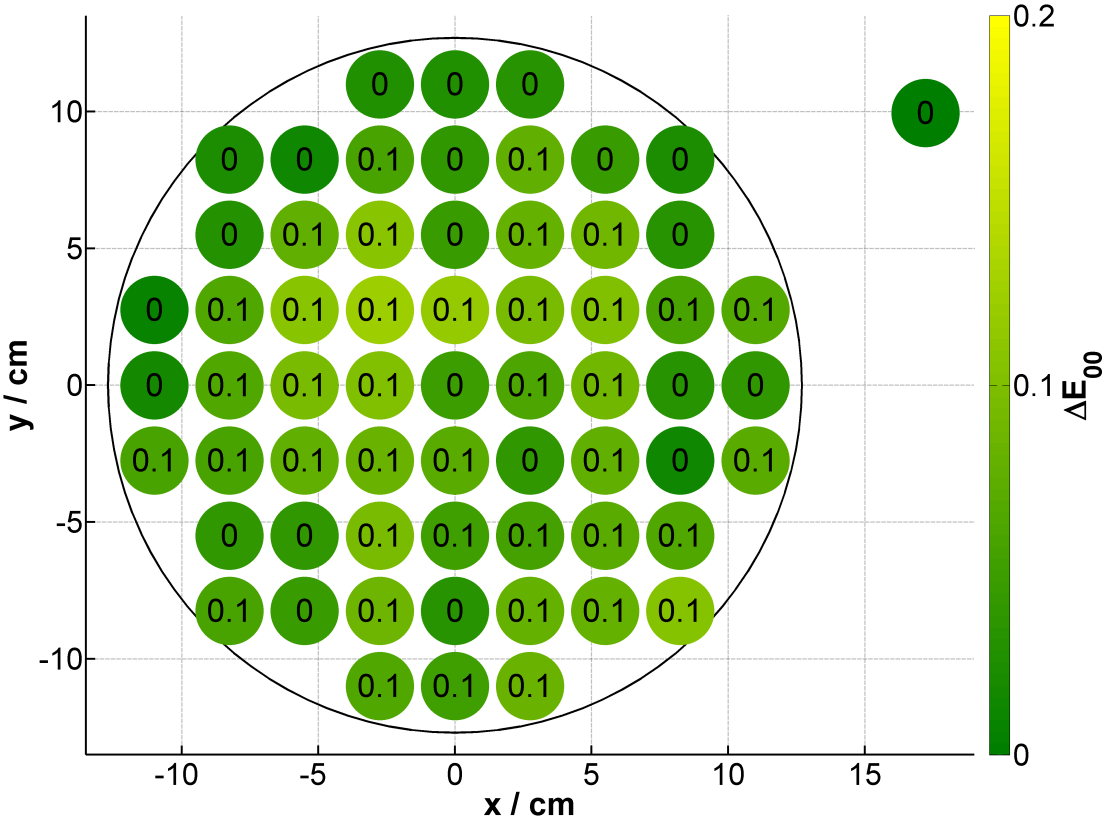

Figure 5.5.: Homogeneity measurement with a 2800 K halogen lamp (H3-2800-778). The data points represent the colour difference ΔE_{00} to the probe port.

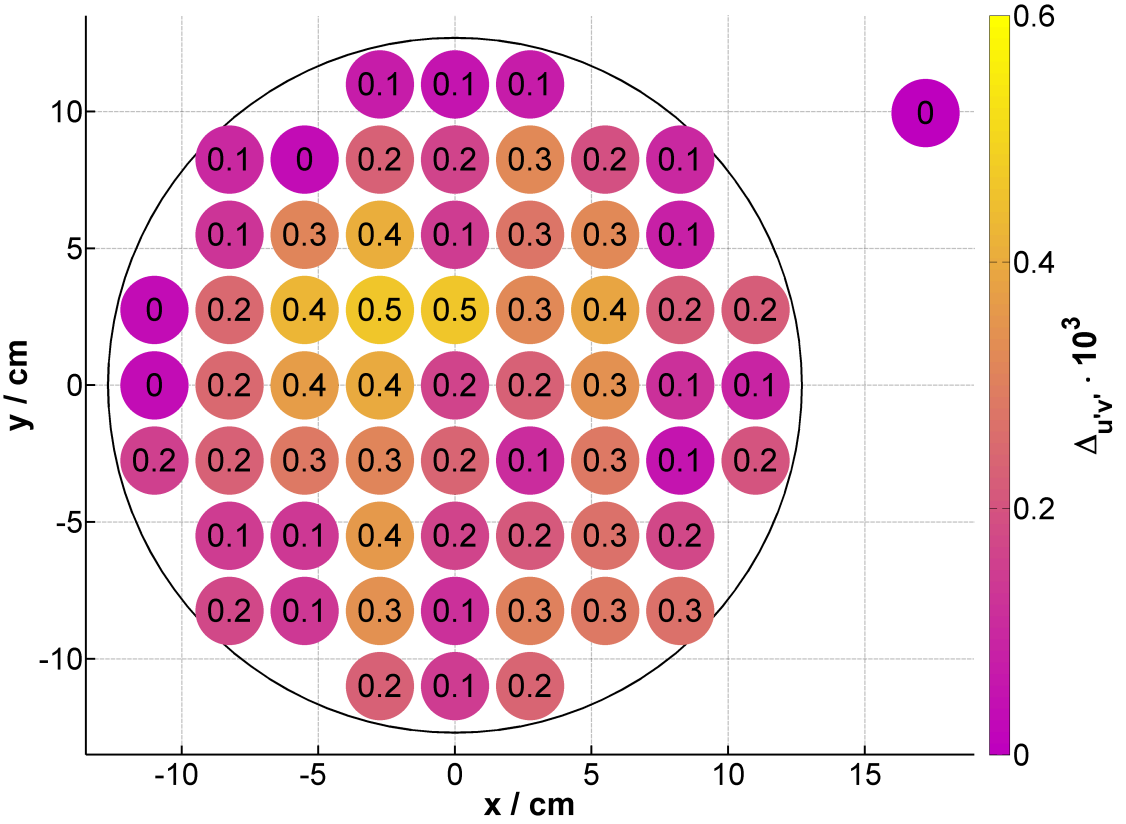

Figure 5.6.: Homogeneity measurement with a 2800 K halogen lamp (H3-2800-778). The data points represent the colour difference $\Delta_{u'v'}$ to the probe port.

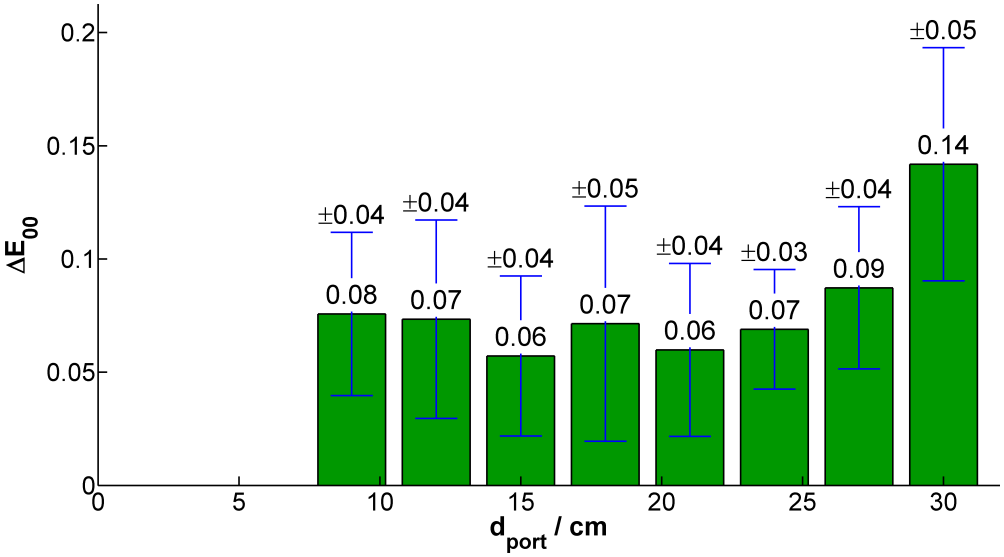

Figure 5.7.: Distribution of the colour difference ΔE_{00} using a 4000 K fluorescent lamp (ES4-4000-740). d_{port} gives the distance to the probe port.

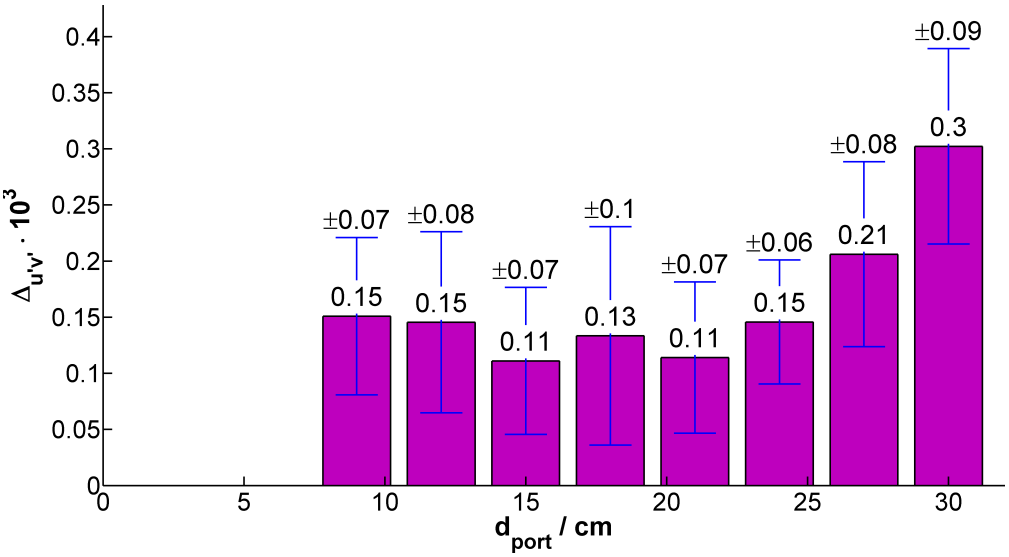

Figure 5.8.: Distribution of the colour difference $\Delta_{u'v'}$ using a 4000 K fluorescent lamp (ES4-4000-740). d_{port} gives the distance to the probe port.

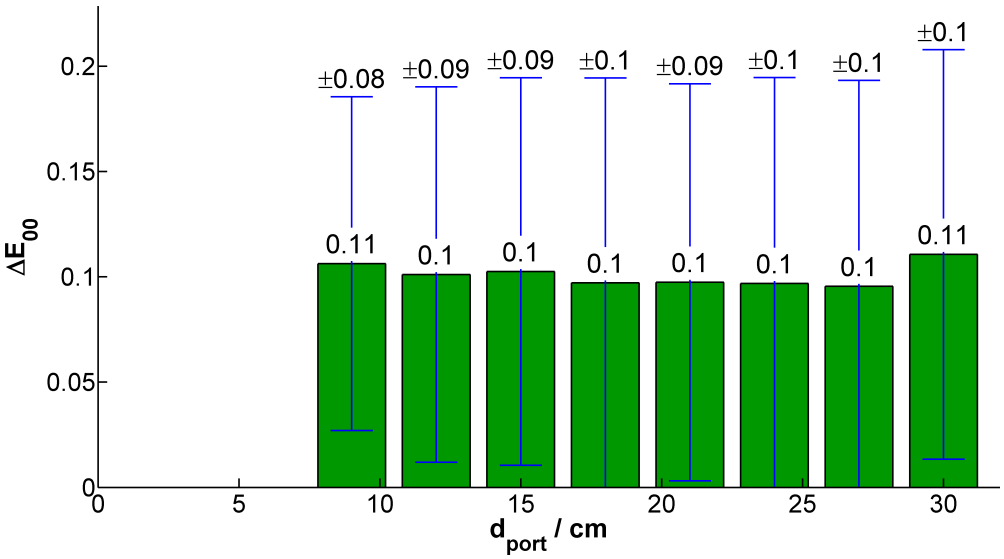

Figure 5.9.: Distribution of the colour difference ΔE_{00} using a 2700 K LED lamp (LED1-2700-806). d_{port} gives the distance to the probe port.

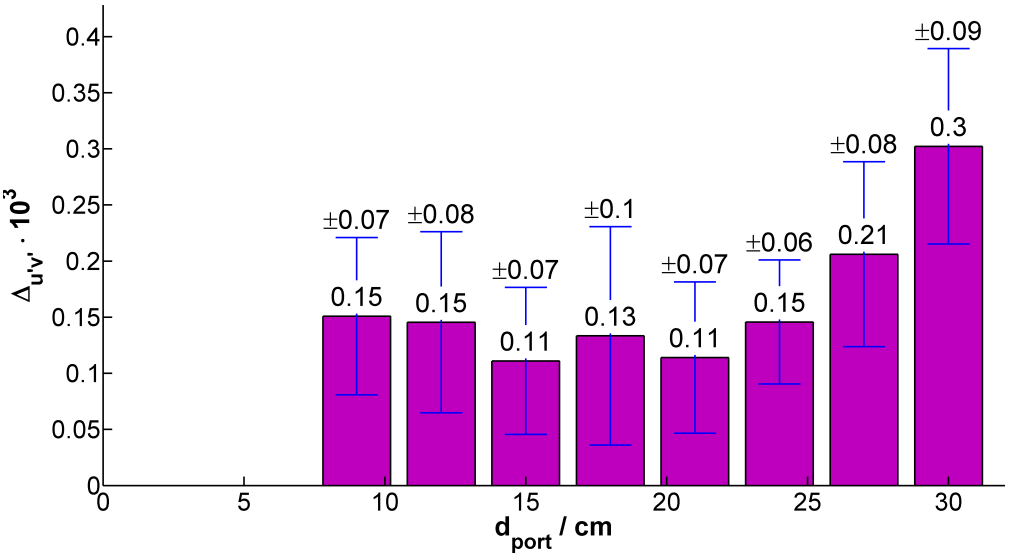

Figure 5.10.: Distribution of the colour difference $\Delta_{u'v'}$ using a 2700 K LED lamp (LED1-2700-806). d_{port} gives the distance to the probe port.

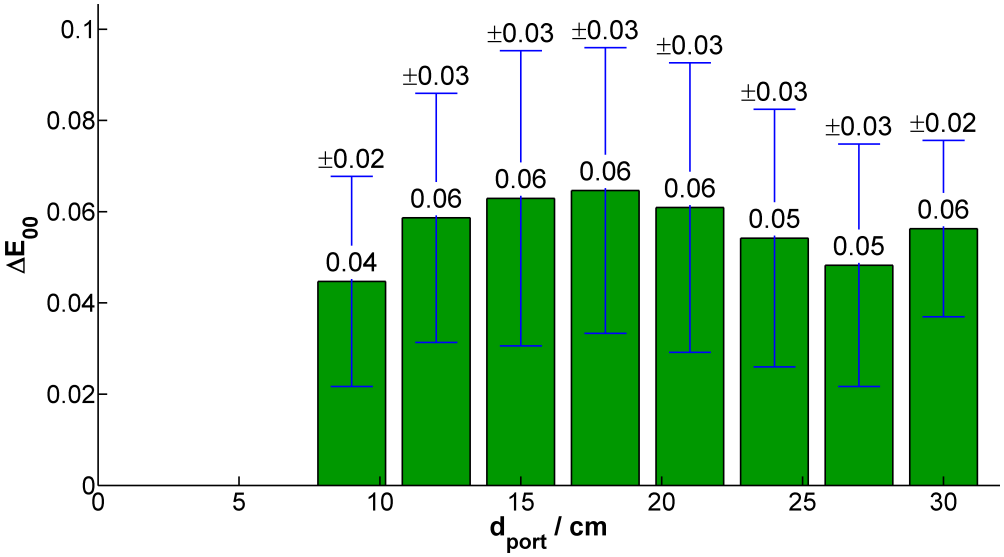

Figure 5.11.: Distribution of the colour difference ΔE_{00} using a 2800 K fluorescent lamp (H3-2800-778). d_{port} gives the distance to the probe port.

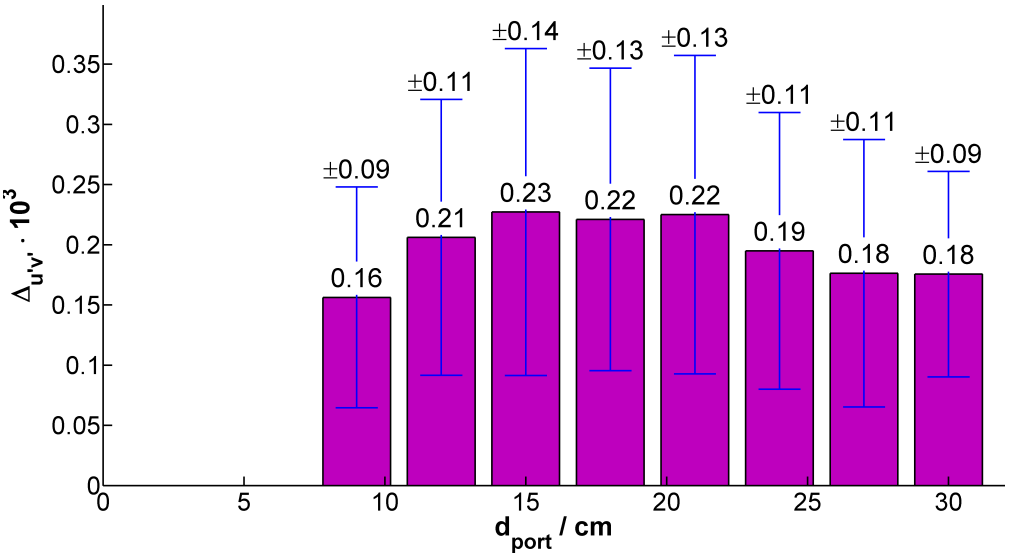

Figure 5.12.: Distribution of the colour difference $\Delta_{u'v'}$ using a 2800 K fluorescent lamp (H3-2800-778). d_{port} gives the distance to the probe port.

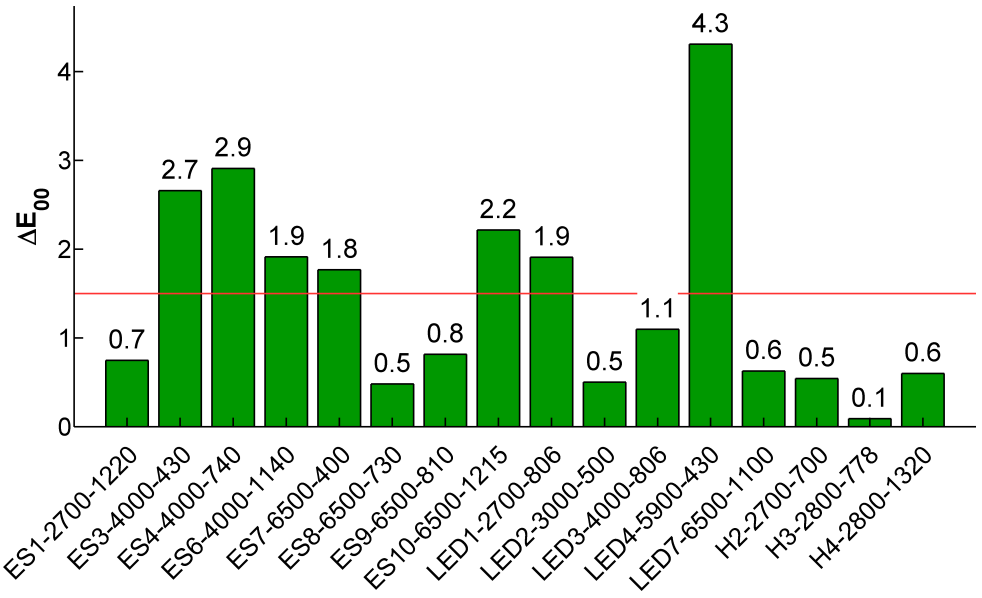

Figure 5.13.: Colour difference ΔE_{00} between the measurements of a calibrated DUT and the reference spectrometer. 16 lamps were used for the calibration. The red line indicates the requested limit for $\Delta E_{00} < 1.5$.

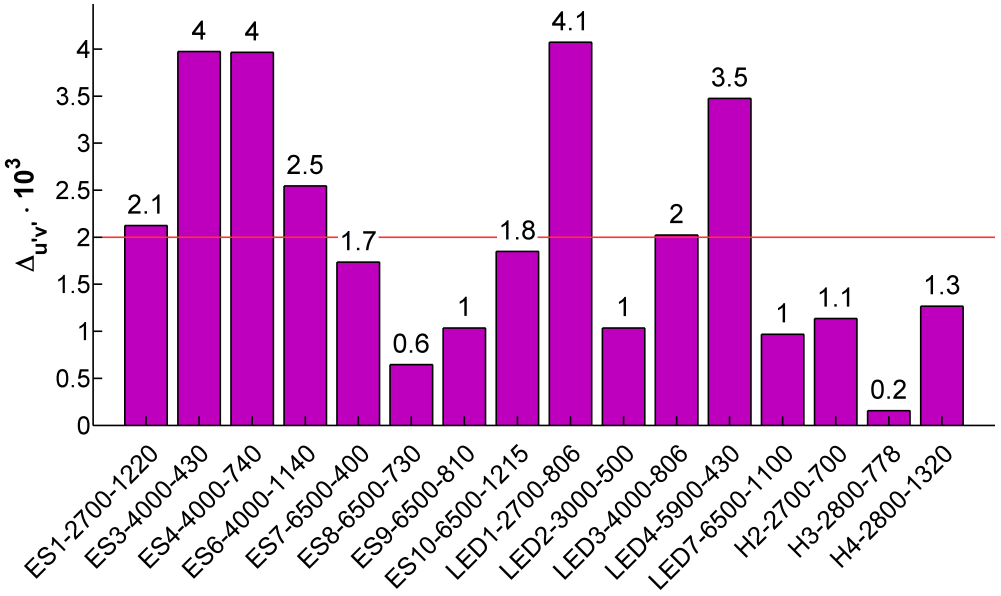

Figure 5.14.: Colour difference $\Delta_{u'v'}$ between the measurements of a calibrated DUT and the reference spectrometer. 16 lamps were used for the calibration. The red line indicates the requested limit for $\Delta_{u'v'} < 2 \cdot 10^{-3}$.

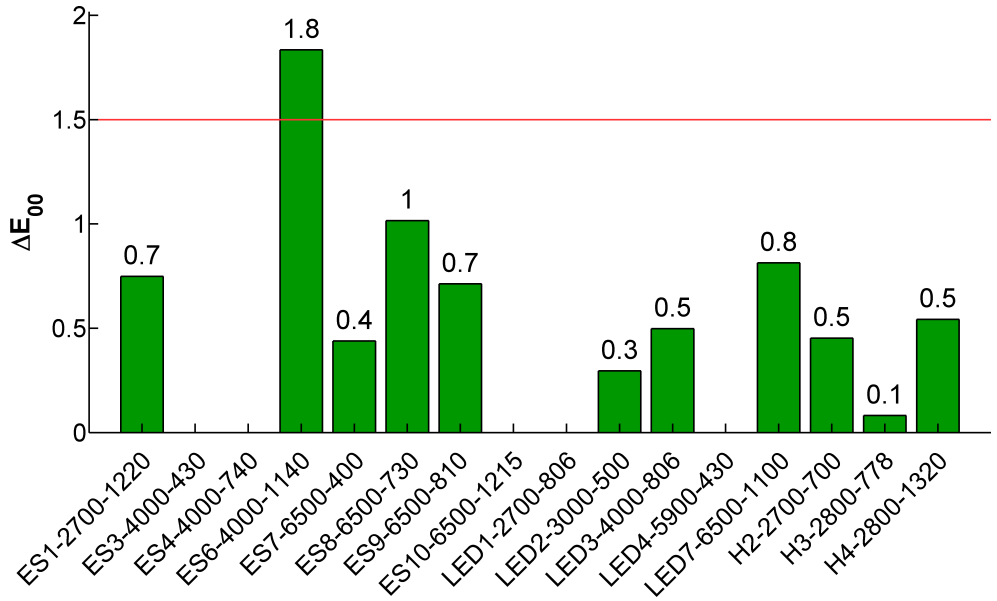

Figure 5.15.: Colour difference ΔE_{00} between the measurements of a calibrated DUT and the reference spectrometer. A deliberate selection of ll lamps was used for the calibration. The red line indicates the requested limit for $\Delta E_{00} < 1.5$.

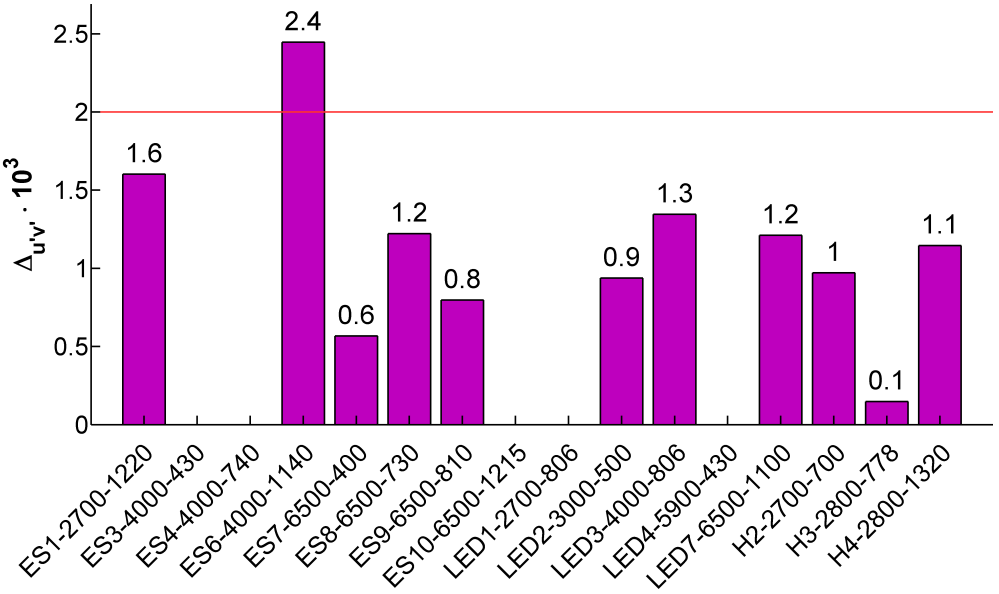

Figure 5.16.: Colour difference $\Delta_{u'v'}$ between the measurements of a calibrated DUT and the reference spectrometer. A deliberate selection of ll lamps was used for the calibration. The red line indicates the requested limit for $\Delta_{u'v'} < 2 \cdot 10^{-3}$.

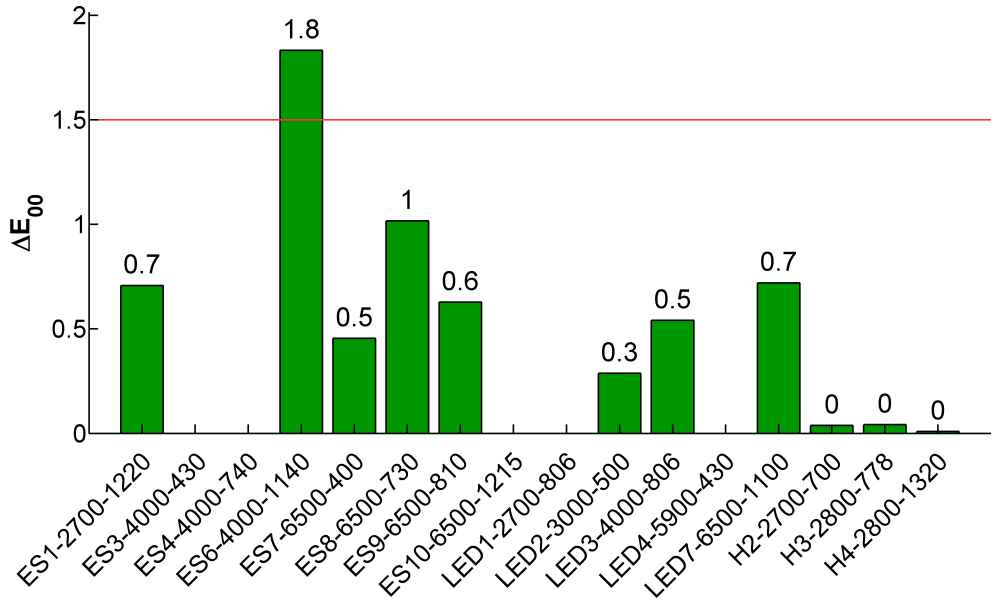

Figure 5.17.: Colour difference ΔE_{00} between the measurements of a calibrated DUT and the reference spectrometer. A deliberate selection of ll lamps and the CCT as fourth channel was used for the calibration. The red line indicates the requested limit for $\Delta E_{00} < 1.5$.

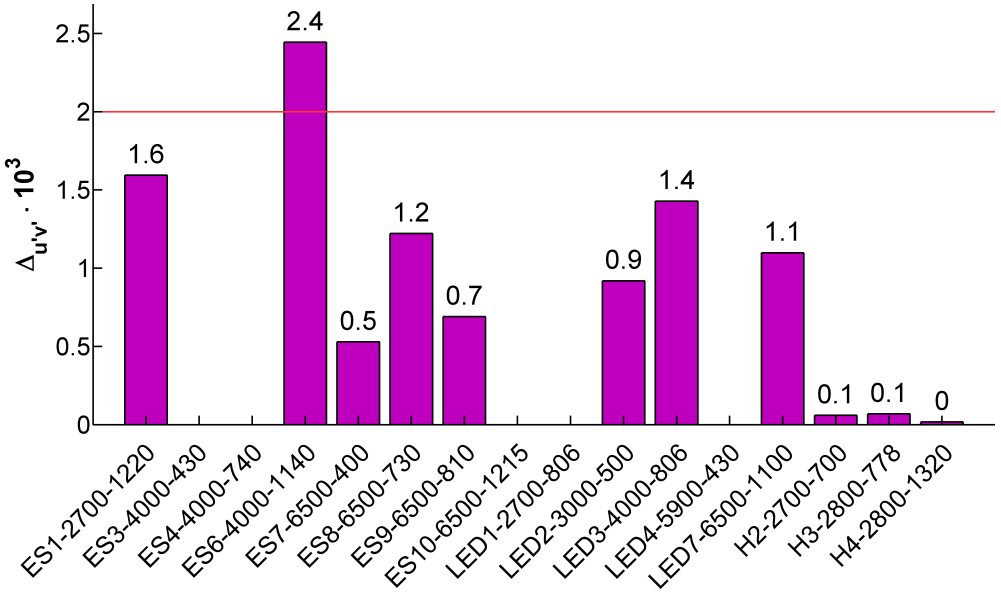

Figure 5.18.: Colour difference $\Delta_{u'v'}$ between the measurements of a calibrated DUT and the reference spectrometer. A deliberate selection of ll lamps and the CCT as fourth channel was used for the calibration. The red line indicates the requested limit for $\Delta_{u'v'} < 2 \cdot 10^{-3}$.

6. Accuracy assessment

The wavelength accuracy of the spectrometer is $\pm 0.3\,\mathrm{nm}$ with a spectroradiometric accuracy of $\pm 3.5\,\%$ [4]. The latter value may seem to be large. But this always means that the whole spectrum is measured stronger or weaker. For colour calculations the relative intensity of the wavelength segments is important. A magnitude for the inaccuracy of the colour point is difficult to obtain since it depends on the region of the colour point.

All the spectrometer measurements in this thesis are regarded as absolute and no inaccuracy is considered. This is legitimized by the fact that the spectrometers accuracy is far better then the one of a colour sensor.

For a best possible diffusity, light rays must travel to all directions and reflect multiple times without getting absorbed. All the baffles explained in section 3.1.2 support this behaviour, but the lamp-frame (see section 3.2.1) doesn't. In production test the lamp-frame should be coated with the reflective paint as well. For the case that it's eliminated and the lamps are fixed on the sphere directly the decrease of sphere area should be compensated. Well considered obstacles covered in reflective paint might improve the diffusity.

Another factor counteracting the diffusity is the different design of the lamps. The angle dependent intensity distribution varies for different lamp types and designs. When the light rays are reflected often enough before hitting the exit port this doesn't matter. But since the exit port is large it is a matter that must be kept in mind.

6.1. Colour homogeneity

Since the colour homogeneity in the light exit port plain is the major factor under investigation, a closer look into the accuracy is taken. To obtain measurement values of sufficient quantity for statistic evaluation nine homogeneity measurements were repeated under the same conditions. That means there were $N = 9$ measurements for each coordinate point. The measurements are from now on referenced with the index $i = \{1, ..., N\}$ for each round. $P_{ref,i}$ refers to measurements taken at the reference point (probe port) and $P_{x,y,i}$ to those taken in the light exit port plain at the respective x and y coordinate.

$$P_{ref,i} = (X, Y, Z)_{ref,i} \tag{6.1}$$

$$P_{x,y,i} = (X, Y, Z)_{x,y,i} \tag{6.2}$$

The tristimulus colour space is not equidistant in terms of colour difference. Therefore

the statistic evaluation is performed using a magnitude of colour difference referred to as ΔC (either ΔE_{00} or $\Delta_{u'v'}$). Still we need a starting point to calculate the colour difference to. For this single case the arithmetic mean $\overline{P}_{ref}$ is used in the tristimulus colour space. Even though this is actually wrong, the effects are very small since the colour points are so close together. Besides that the inaccuracy of this calculation is added to all resulting values at the end.

$$\overline{P}_{ref} = \frac{1}{N}\left(\sum_i X_i\,,\,\sum_i Y_i\,,\,\sum_i Z_i\right)_{ref} \tag{6.3}$$

Now that we have a reference colour point $\overline{P}_{ref}$ the colour difference to every other point is calculated. This is done for the measurements in the light exit port plain $P_{x,y,i}$ as well as for the reference measurements $P_{ref,i}$.

$$\Delta C_{ref,i} = \Delta C\left(\overline{P}_{ref}\,,\,P_{ref,i}\right) \tag{6.4}$$
$$\Delta C_{x,y,i} = \Delta C\left(\overline{P}_{ref}\,,\,P_{x,y,i}\right) \tag{6.5}$$

In section 5.1 the distribution of colour differences ΔC is mapped to the distance to the reference point $d_{ref,i}$. This value is calculated for every pair of coordinates (x, y).

$$d_{ref,i} = \left\|(x,y)_i - (x,y)_{ref}\right\| \tag{6.6}$$
$$\Delta C_{d,i} = \Delta C_{x,y,i} \tag{6.7}$$

The distances $d_{ref,i}$ are now divided into bins. The bin_{min} and bin_{max} values can be chosen arbitrarily.[1] The reference measurements form their own bin. $\Delta C_{ref,i}$.

$$\Delta C_{bin} = \{\Delta C_{d,i}\} \qquad \text{with } bin_{min} < d_{ref,i} < bin_{max} \tag{6.8}$$
$$\Delta C_{ref} = \{\Delta C_{ref,i}\} \tag{6.9}$$

For all bins, including the reference measurement bin, the arithmetic mean and standard deviation are calculated.

$$\overline{\Delta C}_{bin} = AM\left(\Delta C_{bin}\right) \tag{6.10}$$
$$\sigma_{bin} = SD\left(\Delta C_{bin}\right) \tag{6.11}$$
$$\overline{\Delta C}_{ref} = AM\left(\Delta C_{ref}\right) \tag{6.12}$$
$$\sigma_{ref} = SD\left(\Delta C_{ref}\right) \tag{6.13}$$

Finally the arithmetic mean $\overline{\Delta C}_{ref}$ and the standard deviation σ_{ref} of the reference bin are added to the standard deviation of all other bins.

[1] Eight bins from 8 to 30 cm with a width of 5.5 cm have turned out to to give decent results.

$$\sigma_{bin\_total} = \sigma_{bin} + \overline{\Delta C}_{ref} + \sigma_{ref} \tag{6.14}$$

Through this the colour point $\overline{P}_{ref}$ can be regarded as absolute and it's inaccuracy is considered in σ_{bin_total}.

The colour difference distributions in section 5.1 now show the bins at the position of their distance to the reference point. Their size is determined by $\overline{\Delta C}_{bin}$ and the corresponding error bar shows σ_{bin_total}.

6.2. DUT calibration

Through regarding the spectrometer measurements as absolute there is no need for any additional accuracy assessment of the DUT calibration process. The colour difference explained in section 2.3 is a measure for the calibration quality. The reason for inaccuracies come from the sensor itself and are therefore diverse.

7. Conclusion and prospects

In this thesis the capability of an integrating sphere to produce a homogeneously illuminated plane was investigated. Especially homogeneous colour (chromaticity) was of importance and the lightness (illuminance) was neglected. The homogeneously illuminated plain should provide equivalent measurement points for the calibration of ambient light colour sensors. Under the equal light conditions the sensors can then be calibrated simultaneously using only one reference spectrometer.

The homogeneous illumination of the sensor plain turned out quite successful. Measurement values generally fell below the limits of $\Delta E_{00} < 1.5$ and $\Delta_{u'v'} < 2 \cdot 10^{-3}$ by a factor of 10 (see figure 5.7 to 5.12). The standard deviation was about 50% of the colour difference, which is acceptable for low values. Further improvement of the homogeneity could be acquired by using a tube with the sphere radius between the integrating hemispheres. Another possibility is to implement a smaller sphere coated on the outside. The angle-independence and the increase of reflective area of both adaptions eventually support the diffusiveness. Homogeneity improvement without sphere adaptations could be acquired by putting more attention to the lamp design. Due to the large port, different light intensity distributions of the lamps might also have negative effects.

The calibration process works best when the sensors receive about the same illuminance for all measurements (see section 2.4). Unfortunately dimming different lamp types comes with a lot of difficulties. At first the lamps behave already differently when switched on, second they hardly behave predictably when dimmed. An implication of that might be to use only LED lamps for dimming because of their good dimming behaviour and their short reaction time. Other lamps might operate with full luminous power. Different spectra can even be emulated by LEDs. The company *Gamma Scientific* already achieved impressive results with this approach [3].

The attempt with the least effort is to combine the lamps in a way that they achieve equal luminous power in equal times. For this even multiple same lamps can be used and operated on one channel as if they were only one lamp.

The most elegant and still easy solution might be to measure the illuminance constantly after switching on the lamps. Then, as soon as it exceeds a certain value, the sensor measurements are done. This will result in different measurement times for different lamps. It has to be tested if the equal lightness improves the calibration significantly in comparison the operation used in this thesis.

Essential for the calibration of a sensor that must be prepared for various light conditions is the selection of lamps. Of course the sensor will predict the light conditions

best when it was calibrated with similar conditions. Due to the nature of the least squares method, that is used for calibration in this thesis, equal lamps will bias the calibration. Keeping in mind that fluorescent lamps are tough to sense correctly this biasing can be seen in figure 5.13 and 5.14. A more elaborate selection with even less lamps led to much better results (see figure 5.15 and 5.16). An implication of the behaviour seen is that using lots of different lamps doesn't necessarily simplify the calibration process. The selection should be equally distributed concerning colour temperature and lamp type.

Better calibration can not only be achieved by using more sensor channels. Unfortunately this was not tested in this thesis. Improvement can also be accomplished by a transformation of the available channels. It was tried to use the correlated colour temperature as additional sensor channel and the results generally improved, especially for incandescent lamps (see figure 5.17 and 5.18).

In conclusion the homogeneity measurements as well as the sensor calibration turned out to be satisfactory. For both there are numerous options for improvement in prospect. The most fundamental influence remains to be the sensor itself. When the sensor is capable of measuring fine improvement changes they are surely worth approaching.

A. Theory

A.1. CIEDE2000 colour difference: ΔE_{00}

The following algorithm has been taken from [8, 7]. L, a and b stand for the variables used in the CIELAB colour space. All other variables only refer to this algorithm.

$$\Delta E_{00} = \sqrt{\left(\frac{\Delta L'}{K_L S_L}\right)^2 + \left(\frac{\Delta C'}{K_C S_C}\right)^2 + \left(\frac{\Delta H'}{K_H S_H}\right)^2 + R_T \left(\frac{\Delta C'}{K_C S_C}\right)\left(\frac{\Delta H'}{K_H S_H}\right)} \tag{A.1}$$

$$\overline{L}' = (L_1 + L_2)/2 \tag{A.2}$$

$$\overline{C} = (C_1 + C_2)/2 \qquad \text{with} \qquad C_i = \sqrt{a_i^2 + b_i^2} \qquad (i = 1, 2) \tag{A.3}$$

$$\overline{C}' = \left(C_1' + C_2'\right)/2 \qquad \text{with} \qquad C_i' = \sqrt{a_i'^2 + b_i'^2} \qquad (i = 1, 2) \tag{A.4}$$

$$G = \frac{1}{2}\left(1 - \sqrt{\frac{\overline{C}^7}{\overline{C}^7 + 25^7}}\right) \tag{A.5}$$

$$a_i' = a_i\,(1 + G) \qquad (i = 1, 2) \tag{A.6}$$

$$h_i' = \begin{cases} \tan^{-1}(b_i/a_i') & \text{if } \tan^{-1}(b_i/a_i') \geq 0 \\ \tan^{-1}(b_i/a_i') + 360° & \text{otherwise} \end{cases} \qquad (i = 1, 2) \tag{A.7}$$

$$\overline{H}' = \begin{cases} (h_1' + h_2' + 360°)/2 & \text{if } |h_1' - h_2'| > 180° \\ (h_1' + h_2')/2 & \text{otherwise} \end{cases} \tag{A.8}$$

$$\begin{aligned} T = 1 &- 0.17\cos\left(\overline{H}' - 30°\right) + 0.24\cos\left(2\overline{H}'\right) + \ldots \\ \ldots &+ 0.32\cos\left(3\overline{H}' + 6°\right) - 0.20\cos\left(4\overline{H}' - 63°\right) \end{aligned} \tag{A.9}$$

$$\Delta h' = \begin{cases} h'_2 - h'_1 & \text{if } |h'_2 - h'_1| \leq 180^\circ \\ h'_2 - h'_1 + 360^\circ & \text{else if } |h'_2 - h'_1| > 180^\circ \text{ and } h'_2 \leq h'_1 \\ h'_2 - h'_1 - 360^\circ & \text{otherwise} \end{cases} \tag{A.10}$$

$$\Delta L' = L_2 - L_1 \tag{A.11}$$

$$\Delta C' = C'_2 - C'_1 \tag{A.12}$$

$$\Delta H' = 2\sqrt{C'_1 C'_2}\sin\left(\Delta h'/2\right) \tag{A.13}$$

$$S_L = 1 + \frac{0.015\left(\overline{L}' - 50\right)^2}{\sqrt{20 + \left(\overline{L}' - 50\right)^2}} \tag{A.14}$$

$$S_C = 1 + 0.045\,\overline{C}' \tag{A.15}$$

$$S_H = 1 + 0.015\,\overline{C}'T \tag{A.16}$$

$$\Delta\theta = 30\exp\left\{-\left(\frac{\overline{H}' - 275^\circ}{25}\right)^2\right\} \tag{A.17}$$

$$R_C = 2\sqrt{\frac{\overline{C}^7}{\overline{C}^7 + 25^7}} \tag{A.18}$$

$$R_T = -R_C\sin\left(2\Delta\theta\right) \tag{A.19}$$

$$K_L = K_C = K_H = 1 \qquad \text{(default)} \tag{A.20}$$

B. Experimental details

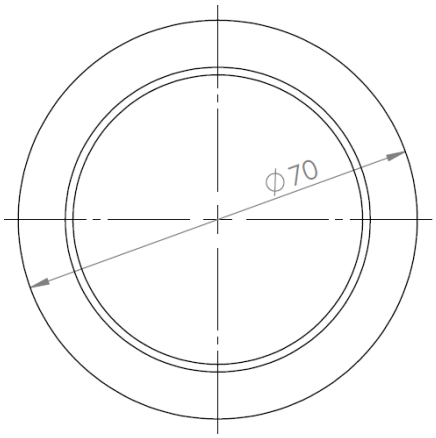

(a) Top view of the port. The diameter is stated for the utmost circle.

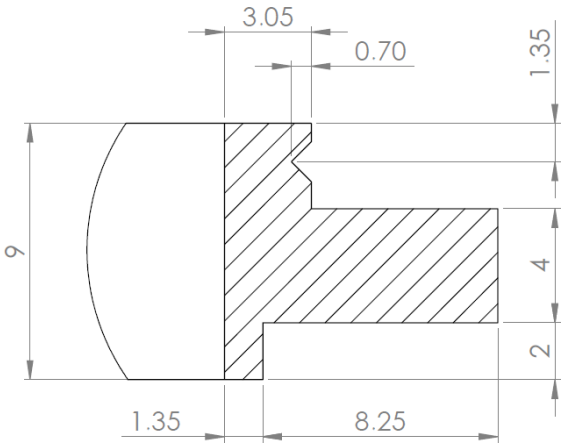

(b) Cutaway view of the port.

Figure B.1.: Spectrometer and cable port *UMPF-2.0*. All units are millimetres.

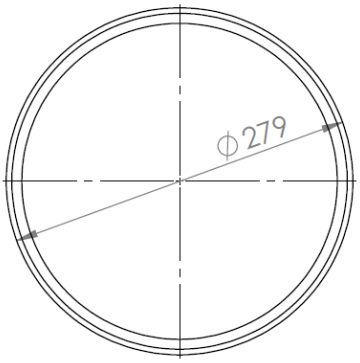

(a) Top view of the port. The diameter is stated for the utmost circle.

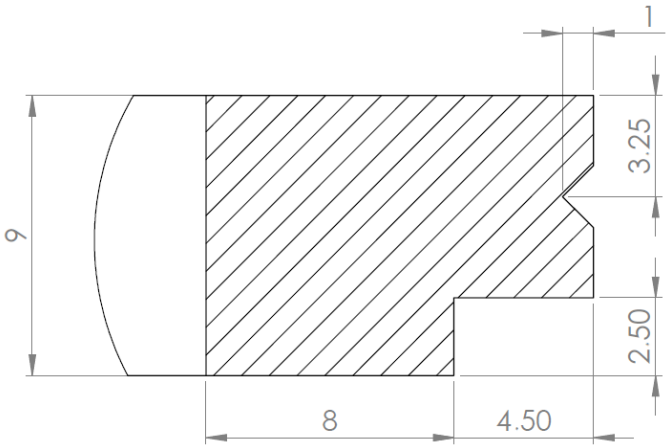

(b) Cutaway view of the port.

Figure B.2.: Light exit port *UMPF-10.0*. All units are millimetres.

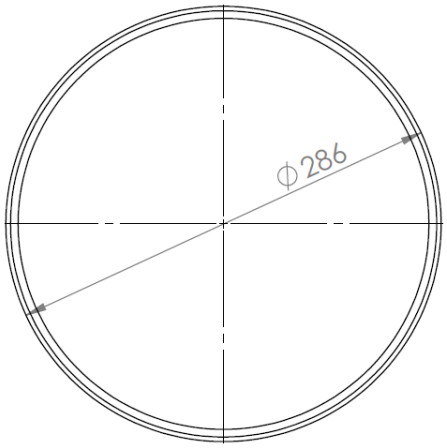

(a) Top view of the plate holder. The diameter is stated for the utmost circle.

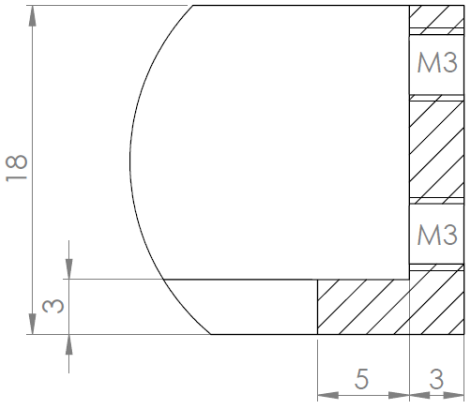

(b) Cutaway view of the plate holder. The top M3 drill hole is to fix the holder on the light exit port notch. The bottom one is to fix an inset plate.

Figure B.3.: Plate holder for light exit port. All units are millimetres.

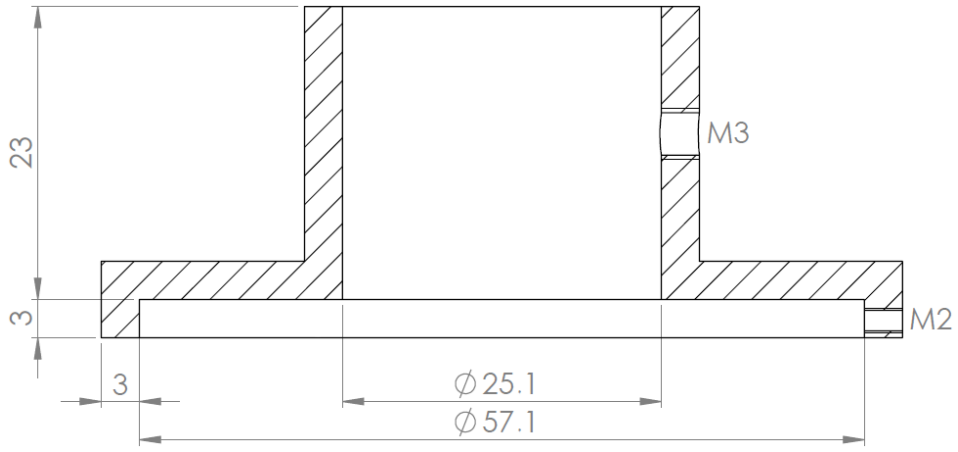

Figure B.4.: Cutaway view of the spectrometer probe adapter. The M2 drill holes are to fix the adapter on the spectrometer port notch. There are three arranged 120° apart around the middle axis. The M3 drill hole provides fixation for the spectrometer probe. All units are millimetres.

Table B.1.: Grid coordinates for the homogeneity measurements.

x . . . x-coordinate

y . . . y-coordinate

x	y	x	y	x	y
mm	mm	mm	mm	mm	mm
0	0				
0	28	83	-27	-55	-27
0	55	83	-55	-82	-27
0	83	83	-82	-82	-55
0	110	55	-82	-82	-82
28	110	55	-55	-110	-27
28	83	55	-27	-110	0
28	55	28	-27	-110	28
28	28	28	-55	-82	83
28	0	28	-82	-82	55
55	0	28	-110	-82	28
55	28	0	-110	-82	0
55	55	0	-82	-55	0
55	83	0	-55	-55	28
83	83	0	-27	-55	55
83	55	-27	-27	-55	83
83	28	-27	-55	-27	110
83	0	-27	-82	-27	83
110	28	-27	-110	-27	55
110	0	-55	-82	-27	28
110	-27	-55	-55	-27	0

Bibliography

[1] Angelo V Arecchi and Tahar Messadi. *Field Guide to Illumination*, volume FG11. 2007. ISBN 9780819481221. doi: 10.1117/3.764682.

[2] CIE. Chromaticity Difference Specification for Light Sources, 2014, `http://files.cie.co.at/738_CIE_TN_001-2014.pdf` (Accessed: 2017-05-01).

[3] Gamma Scientific. Tunable LED Uniform Light Sources, `http://www.gamma-sci.com/products/light_sources/tunable-led/` (Accessed: 2017-06-01).

[4] Instrument Systems. CAS 140CT Array Spectrometer, `http://www.instrumentsystems.com/fileadmin/editors/downloads/Products/CAS140CT_e.pdf` (Accessed: 2017-04-24).

[5] Klaus Jänich. *Lineare Algebra*. Springer-Lehrbuch. Springer, Berlin, Heidelberg, 10 edition, 2004. ISBN 3-540-40207-7. doi: 10.1007/978-3-662-08375-8.

[6] Douglas A Kerr. A Metric for Chromaticity Difference, 2008, `http://dougkerr.net/Pumpkin/articles/Chromaticity_Metric.pdf` (Accessed: 2017-05-01).

[7] Bruce Lindbloom. www.brucelindbloom.com, `http://www.brucelindbloom.com/` (Accessed: 2017-04-29).

[8] Gaurav Sharma, Wencheng Wu, and Edul N Dalal. The CIEDE2000 Color-Difference Formula: Implementation Notes, Supplementary Test Data, and Mathematical Observations, 2005, `http://www.ece.rochester.edu/$\sim$gsharma/ciede2000/ciede2000noteCRNA.pdf` (Accessed: 2017-05-01).

[9] Thorlabs. 300 mm Linear Translation Stage with Integrated Controller, Stepper Motor, `https://www.thorlabs.com/newgrouppage9.cfm?objectgroup_id=7652&pn=LTS300` (Accessed: 2017-04-27).